

Low valent transition metal clusters containing nitrene/imido ligands

Yat Li, Wing-Tak Wong*

Department of Chemistry, The University of Hong Kong, Pokfulam Road, Hong Kong

Received 12 December 2002; accepted 24 April 2003

Contents

| | |
|----------------------------------------------------------------------------|-----|
| 1. Introduction | 192 |
| 2. Synthetic methodologies | 192 |
| 2.1 Homometallic complexes | 193 |
| 2.1.1 Use of nitro/nitroso compounds | 193 |
| 2.1.2 Use of azide compounds | 193 |
| 2.1.3 Use of organonitrile compounds | 193 |
| 2.1.4 Use of azo compounds | 193 |
| 2.1.5 Use of amino compounds | 194 |
| 2.1.6 Use of isocyanate and thionylaniline compounds | 194 |
| 2.1.7 Use of nitrido compounds | 194 |
| 2.1.8 Use of nitrosyl compounds | 194 |
| 2.1.9 Others | 194 |
| 2.2 Heterometallic complexes | 195 |
| 2.2.1 Use of nitrosyl compounds | 196 |
| 2.2.2 Use of nitrido mixed-metal clusters | 196 |
| 2.2.3 Use of imido metal clusters | 196 |
| 3. Structural properties | 196 |
| 3.1 d ⁸ Transition metal cluster series (Fe, Ru and Os) | 196 |
| 3.2 d ⁹ Transition metal cluster series (Co and Rh) | 198 |
| 3.3 Other transition metal clusters | 199 |
| 3.4 Heterometallic transition metal clusters | 199 |
| 4. NMR spectroscopic properties of (μ_3 or μ_4 -NH) imido ligands | 200 |
| 4.1 ^{4,11} H-NMR spectroscopy | 200 |
| 4.2 ^{4,215} N-NMR spectroscopy | 202 |
| 5. Reactivities | 203 |
| 5.1 Reactions toward alkynes | 203 |
| 5.2 Reactions toward azo compounds | 205 |
| 5.3 Reductive reactions | 206 |
| 5.4 Other reactions | 208 |
| 6. Electrochemical studies | 208 |
| 7. Catalytic properties | 209 |
| 8. Concluding remarks | 210 |
| Acknowledgements | 211 |
| References | 211 |

Abstract

This short review describes the synthesis, structural and spectroscopic properties, and reactivity studies of low valent transition metal clusters that contain nitrene/imido ligands. The synthetic routes to these nitrene/imido-capped transition metal clusters (both homometallic and heterometallic) are generalized. Numerous structures of these species have been established by X-ray

* Corresponding author. Tel.: +852-28592157; fax: +852-25472933.

E-mail address: wtwong@hkuc.hku.hk (W.-T. Wong).

crystallography in recent decades. Their geometric features, which are governed by the capping ligands and metal atoms, are described, and the ^1H - and ^{15}N -NMR studies of these clusters with (μ_3 - or μ_4 -NH) nitrene ligands are highlighted. The different degrees of interaction of nitrogen atoms with metals in μ_4 -NH and μ_3 -NH bonding modes result in distinct NMR parameters. The influences of the coordinated ligands and metal atoms on the NH proton signal are also discussed. The electrochemical responses of these clusters are directly related to the nature of the capping ligands, and the addition/reduction of cluster valence electron (CVE) leads to marked changes in the cluster geometry. The μ_3 -imido capped triruthenium metal clusters are known to be the active intermediates in the reductive carbonylation of nitro-compounds. The proposed catalytic mechanisms are discussed.

© 2003 Elsevier B.V. All rights reserved.

Keywords: Nitrene; Imido; Transition metal cluster

1. Introduction

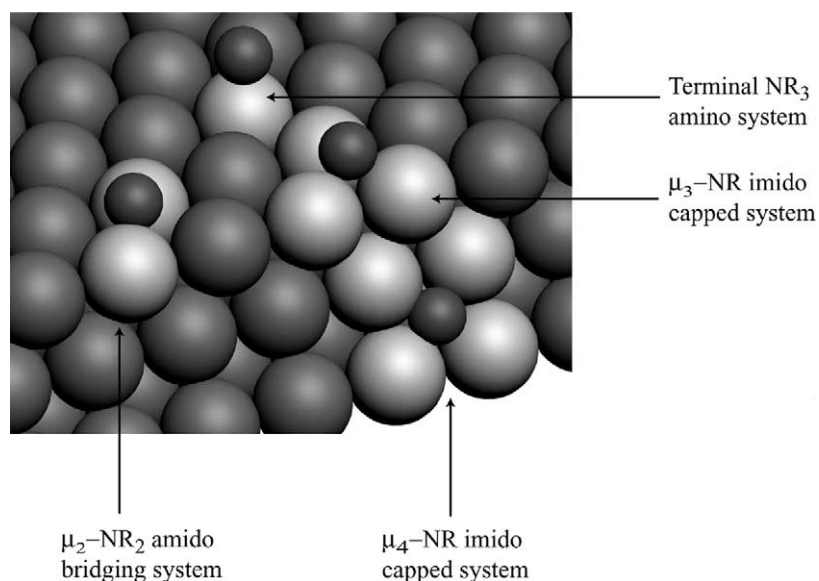
Transition metal clusters with nitrene/imido ligands have been known for a long time, and their chemical reactivity studies are of considerable interest because adsorbed nitrogen atoms are believed to be key intermediates in several industrial chemical processes, such as the Haber process [1–3] and the oxidation of ammonia [4–6]. The bonding correlation between coordinated transition metal clusters and the surface bound NH_x moieties is illustrated in Scheme 1. In the last few decades, numerous low valent transition metal clusters that contain capping nitrene/imido ligands have been prepared and studied. This review provides a short survey of the chemistry of these reported clusters.

The nitrene/imido metal complexes are classified into those species that contain the $\text{M}-\text{NR}$ unit (M = metal). The R group can be hydrogen, alkyl, aryl, alkoxy, or trimethylsilane, which is singly bonded to the basal nitrogen atom. The $\text{M}-\text{NR}$ moieties that contain complexes are termed transition metal–imido or –nitrene, depending on whether the nitrogen is electron

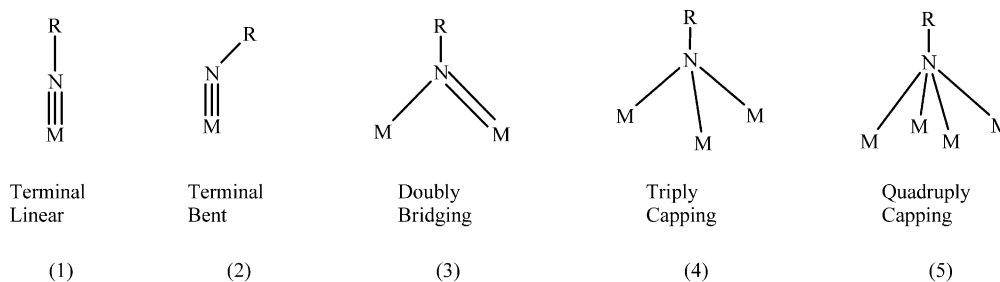
rich or electron deficient. However, in this review, the term ‘imido’ will be used when referring to nitrene and imido species collectively. The five known coordination modes of imido ligands are shown in Scheme 2. The triply and quadruply capping moieties are most commonly observed in the low valent transition metal clusters, which have a low capacity for metal–nitrogen π -bonding, and this is the subject of this review. The high valent metal complexes and the terminal or doubly bridging imido ligands (bonding modes 1–3) will not be covered. Several excellent reviews have been published on such species [7–11].

2. Synthetic methodologies

A number of synthetic routes to imido-capped low-valent transition metal clusters have been studied, and several seem to have some degrees of generality. They are categorized according to the nature of the starting materials.



Scheme 1.



Scheme 2.

2.1. Homometallic complexes

2.1.1. Use of nitro/nitroso compounds

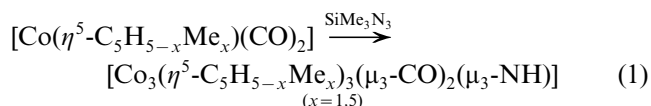
It is well known from the early work of Sappa and Milone that the treatment of $[M_3(CO)_{12}]$ ($M = Fe, Ru$) with nitro compounds (RNO_2) at elevated temperature gives a series of monocapped or bicapped imido metal clusters $[M_3(\mu_3-NR)_x(\mu_3-CO)_y(CO)_9]$ ($x = 1, 2$; $y = 0, 1$; $R = Ph, Et, Me, C_6Cl_5$), accompanied by the formation of CO_2 (Scheme 3) [12]. This suggests that metal carbonyl clusters induce the deoxygenation of nitro compounds to form imido ligands [13–20].

Nitrosobenzene is another promising precursor for the preparation of imido ligands. Cluster anions $[Ru_3(\mu_3-NPh)(X)(CO)_9]^-$ ($X = Cl, Br, I, CN, H$) can be formed rapidly from the reaction between nitrosobenzene and $[Ru_3(\mu-X)(CO)_n]^-$ ($n = 10, 11$) under the promotion of halides, cyanide, or hydride ligands (Scheme 4) [21–24]. $[Ru_3(\mu-X)(CO)_n]^-$ are believed to promote the loss of CO and lead to the formation of an intermediate with coordinated nitrosobenzene, which quickly deoxygenate to form CO_2 and the imido ligand.

2.1.2. Use of azide compounds

In the 1970s Gustorf and Krueger showed that the reaction between $[Fe_2(CO)_9]$ and $[SiMe_3N_3]$ afforded $[Fe_3(CO)_{10}(\mu_3-NSiMe_3)]$ in high yield [25,26]. Thereafter, Abel employed this synthetic strategy to prepare a series of Me_3SiN -capped trinuclear metal clusters (Rh, Co, Ru) [27]. The (μ_3-NH) imido-capped cluster $[Co_3(\eta^5-C_5Me_5)_3(\mu_3-CO)(\mu_3-NH)]$ was also isolated in a similar reaction, where the ligand transformation that

involved a N–Si bond cleavage was observed (Eq. (1)) [28].



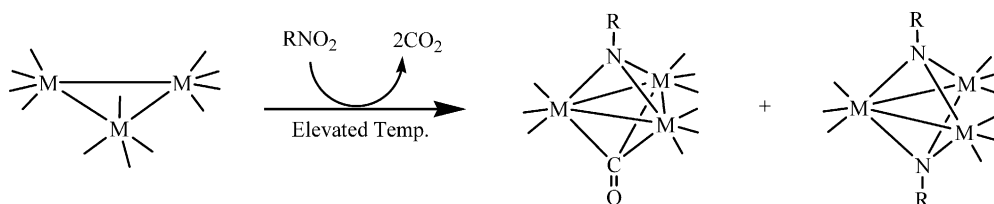
The reactions of either $[Os_3(\mu-H)_2(CO)_{10}]$ or $[Os_3(CO)_{11}(NCMe)]$ with organic azides N_3R ($R = Ph, ^iBu, CH_2Ph, cyclo-C_6H_{11}, PhC=CH_2$) were also reported to afford the complexes $[Os_3(\mu-H)(CO)_{10}(HN_3R)]$. Further thermolysis of these complexes liberated a N_2 and a CO molecule to give imido complexes $[Os_3(\mu-H)_2(CO)_9(\mu_3-NR)]$ (Scheme 5) [29,30].

2.1.3. Use of organonitrile compounds

The hydrogenation of $[Fe_3H(\mu_3-\eta^2-N=CHMe)(CO)_9]$ to give a triply-capped imido cluster $[Fe_3(\mu_3-NEt)(CO)_9]$ was first observed by Kaesz [31]. Mays reported that the reaction of CF_3CN with unsaturated $[Os_3(\mu-H)_2(CO)_{10}]$ afforded the edge-bridged cluster $[Os_3(\mu-H)(CO)_{10}(\mu-N=CHCF_3)]$, which further reacted exhaustively with molecular hydrogen to give $[Os_3(\mu-H)_2(CO)_9(\mu_3-NCH_2CF_3)]$ and $[Os_3H(\mu-H)_3(CO)_8(\mu_3-NCH_2CF_3)]$ (Scheme 6) [32,33]. A similar situation was also observed in the reaction of $[Ru_3(CO)_{12}]$ with *p*-methoxybenzonitrile to yield $[Ru_3(\mu-H)_2(CO)_9(\mu_3-NCH_2C_6H_4OMe)]$ in the presence of acetic acid and molecular hydrogen [34].

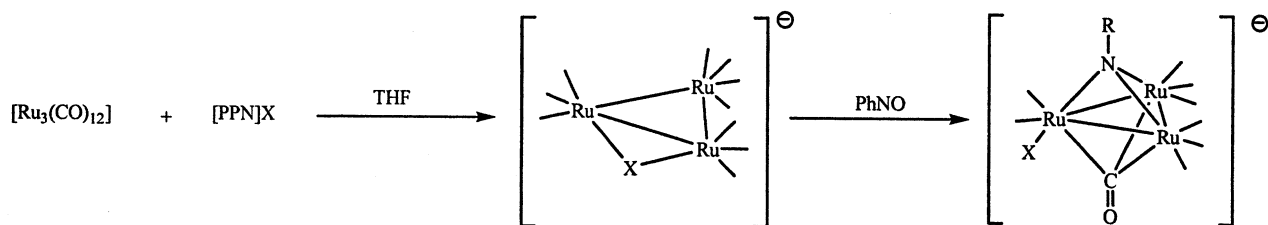
2.1.4. Use of azo compounds

The reaction of azo compounds R_2N_2 ($R = Me, Et, Pr, Ph$) with $[M_3(CO)_{12}]$ ($M = Fe, Ru$) usually results in azo metal complexes $[M_3(CO)_9(\mu_3-\eta^2-R_2N_2)]$. Thermo-



* The terminal carbonyl ligand is denoted by short straight line for clarity

Scheme 3.



Scheme 4.

lysis of these complexes leads to the N–N bond cleavage to form imido-capped clusters $[\text{M}_3(\text{CO})_9(\mu_3\text{-NR})_2]$ (Scheme 7) [35–38]. However, similar reactions have not been observed in the osmium system. Instead the unsaturated osmium clusters $[\text{Os}_3(\mu\text{-H})_2(\text{CO})_{10}]$ reacted with diazobenzene at elevated temperature to give a higher nuclearity imido cluster $[\text{Os}_5(\mu\text{-H})(\text{CO})_{13}(\text{PhNC}_6\text{H}_4\text{N})]$ [39].

2.1.5. Use of amino compounds

$[\text{Ru}_3(\text{CO})_{12}]$ has been reported to catalyze the reduction of nitrobenzene to aniline in which an intermediary imido compound can be isolated [40]. Therefore, the aniline is believed to be able to react with the parent cluster to regenerate the imido intermediate in a reverse reaction. This suggestion is indicated by the formation of $[\text{Os}_3(\mu\text{-H})_2(\text{CO})_9(\mu_3\text{-NPh})]$ from the reaction of $[\text{Os}_3(\text{CO})_{12}]$ and aniline as reported by Deeming (Scheme 8) [41]. In addition, the transformation of tetraosmium amine cluster $[\text{Os}_4(\mu\text{-H})_4(\text{CO})_{11}(\text{NH}_2\text{O}^t\text{Bu})]$ into imido cluster $[\text{Os}_4(\mu\text{-H})_2(\text{CO})_{12}(\mu_3\text{-NH})]$ through amido cluster $[\text{Os}_3(\mu\text{-H})_3(\mu\text{-NH}_2)(\text{CO})_{12}]$ was recently demonstrated by Wong and coworkers (Scheme 9) [42].

2.1.6. Use of isocyanate and thionylaniline compounds

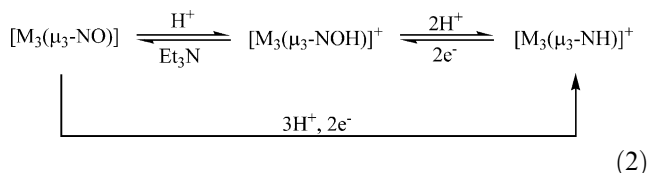
The reactions of $[\text{M}_3(\text{CO})_{12}]$ ($\text{M} = \text{Ru}, \text{Os}$) with the thionylaniline (PhNSO) that afforded several new cluster complexes which contained phenylimido and thio ligands have been reported by Shriver (Scheme 10) [43,44]. Furthermore, the reaction of $[\text{HFe}_3(\text{CO})_{11}]$ with isocyanate (PhNCO) gives the similar phenylimido tri-iron clusters $[\text{Fe}_3(\mu\text{-H})_2(\mu_3\text{-NPh})(\text{CO})_9]$ and $[\text{Fe}_3(\mu_3\text{-NPh})(\mu_3\text{-CO})(\text{CO})_9]$ [45].

2.1.7. Use of nitrido compounds

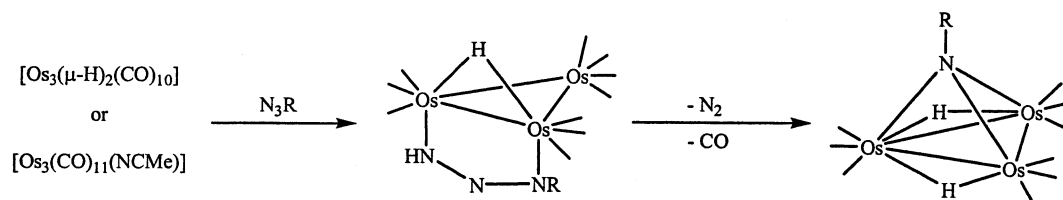
The protonation of nitrido clusters is believed to be one of the most effective synthetic routes for the preparation of NH imido clusters. The reaction of $[\text{PPN}][\text{Fe}_4(\mu_4\text{-N})(\text{CO})_{12}]$ $\{\text{PPN}=(\text{Ph}_3\text{P})_2\text{N}\}$ with acids affords the triply capped imido clusters $[\text{Fe}_3(\mu_3\text{-NH})(\text{CO})_{10}]$ in moderate yield [46,47]. The formation of a quadruply bridging imido cluster seems to be more difficult. The intermediate tetrabridging imido cluster $[\text{Ru}_4(\mu_4\text{-NH})(\text{PhCCPh})(\text{CO})_{11}]$ can be isolated from the reaction of $[(\text{Ph}_3\text{P})_2\text{N}][\text{Ru}_4(\mu_4\text{-N})(\text{CO})_{12}]$ with triflic acid ($\text{CF}_3\text{SO}_3\text{H}$) only in the presence of diphenylacetylene (Scheme 11) [48].

2.1.8. Use of nitrosyl compounds

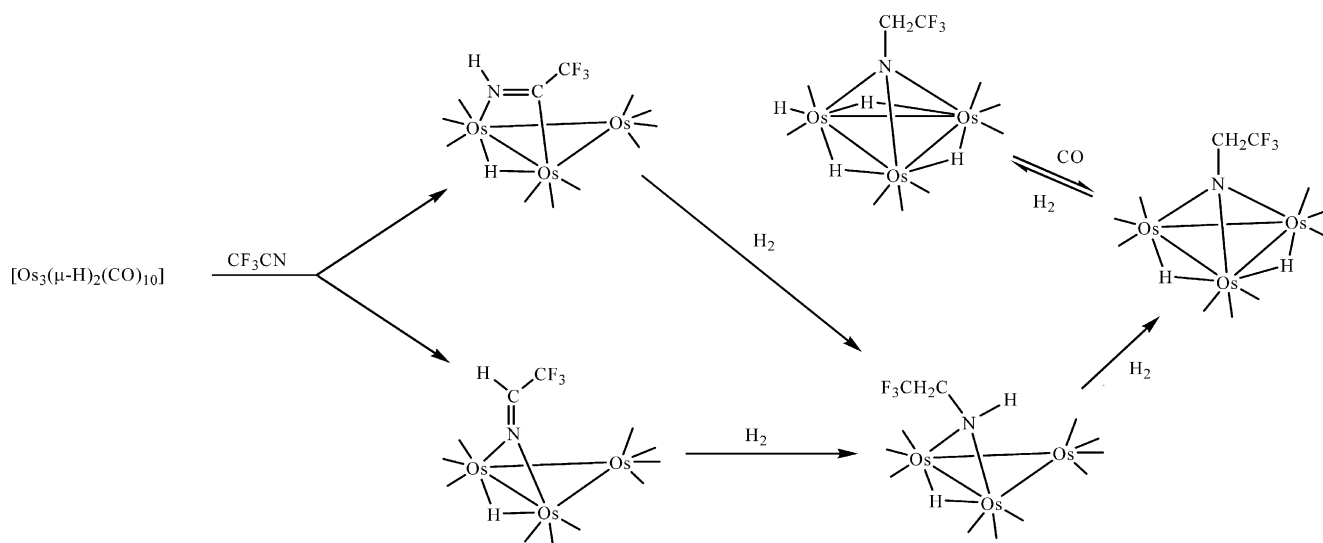
In 1983, Legzdins reported the sequential reduction of $\text{Mn}_3(\mu_3\text{-NO})$ into a $(\mu_3\text{-NH})$ imido ligand with strong protonic acids (Eq. (2)) [49].



This showed that the maximum reduction of the N–O bond order occurs in trinuclear systems $[\text{M}_3(\mu_3\text{-NO})]$ and that the transformation of a NO group to a NH ligand by NO bond cleavage is effective. Recently, the imido cluster $[\text{Ru}_5(\text{CO})_{10}(\mu\text{-CO})_2(\mu_3\text{-CO})(\mu_4\text{-NH})(\mu_3\text{-PN}^i\text{Pr}_2)]$ was also prepared via the treatment of triflic acid with nitrosyl cluster complex $[\text{PPN}][\text{Ru}_5(\text{CO})_{13}(\mu\text{-NO})(\mu_4\text{-PN}^i\text{Pr}_2)]$ [50]. In addition, Wong et al. reported the isolation of a series of novel $(\mu_4\text{-NH})$ imido ligands containing ruthenium carbonyl clusters by the thermolysis or pyrolysis of nitrosyl $(\mu_3\text{-NOMe})$ clusters (Scheme 12) [51–55].



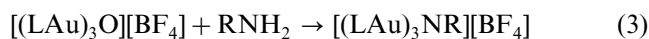
Scheme 5.



Scheme 6.

2.1.9. Others

Apart from the above mentioned synthetic methods, there are other synthetic routes to the imido clusters. However, such routes are usually less common and lack selectivity and cannot be systematically classified. It is noteworthy that the strong aurating agents, which are designed to introduce $[\text{LAu}]^+$ ($\text{L} = \text{PR}_3$) at a given nucleophilic center, can gild the nitrogen atom to give triply bridged imido ligands. Using the reagents, such as $[(\text{LAu})_3\text{O}]^+\text{X}^-$ or $[\text{LAu}]^+\text{X}^-$, primary amines can be converted into ammonium salts $[\text{RN}(\text{AuL})_3]^+\text{X}^-$ with a variety of alkyl or aryl groups (Eq. (3)) [56–61].

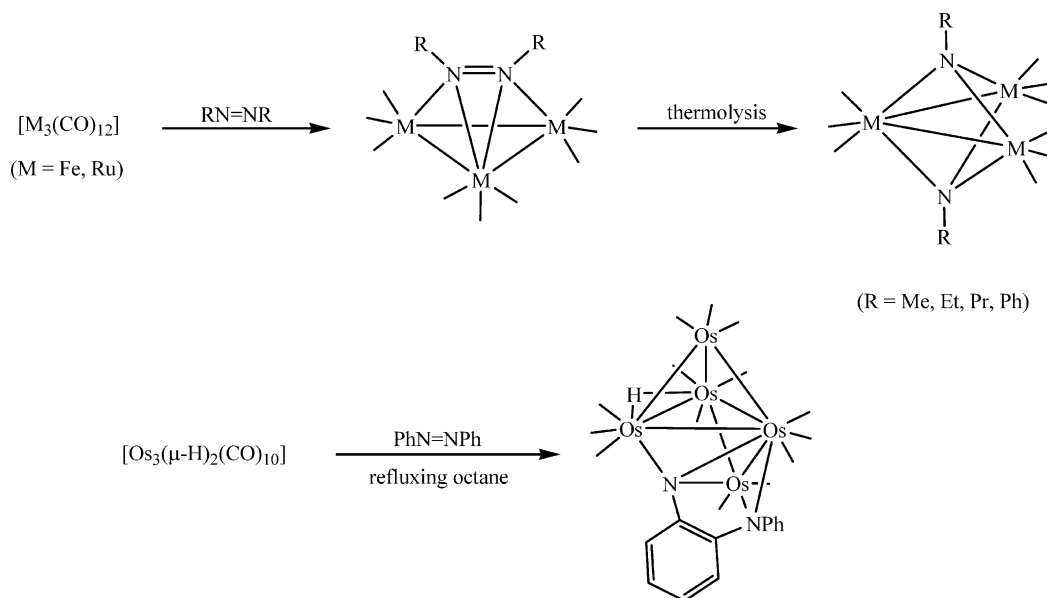


In addition, Watanabe reported that the reaction of

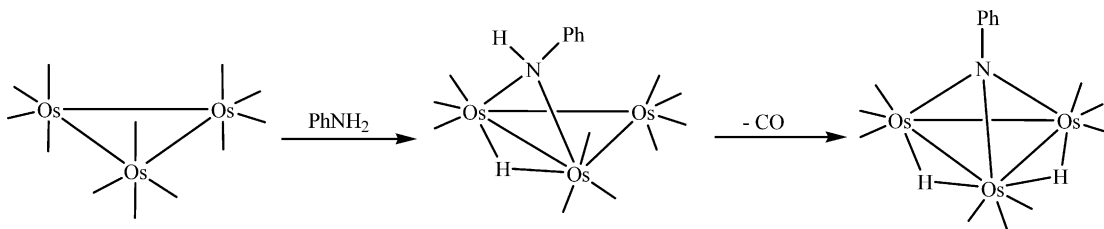
$[(t\text{-C}_4\text{H}_9\text{N})_2\text{S}]$ with $[\text{Cp}_2\text{Ni}]$ ($\text{Cp} = \eta^5\text{-C}_5\text{H}_5$) or $[\text{CpNi}(\text{CO})]_2$ produced the trinuclear imido complex $[t\text{-C}_4\text{H}_9\text{N}(\text{CpNi})_3]$ (Scheme 13) [62,63]. The similar triangulo- Ni_3 core was obtained from the reaction of 2-nitrophenol with $\text{Ni}(\text{PMe}_3)_4$ [64]. Furthermore, Süss-Fink et al. reported the reaction between $[\text{Os}_3(\text{CO})_{12}]$ and $[\text{S}(\text{NSiMe}_3)_2]$, as shown in Scheme 14, which led to the isolation of a triply-bridging imido cluster $[\text{Os}_3(\text{CO})_9(\mu_3\text{-S})(\mu_3\text{-NSiMe}_3)]$ by facile N–S bond cleavage.

2.2. Heterometallic complexes

The chemistry of the imido-capped mixed-metal clusters is also important since mixed-metal clusters



Scheme 7.



Scheme 8.

have been increasingly used in catalysis over the last three decades. There is evidence that the cooperative effects may lead to improved properties when compared to homometallic systems [65–67]. Several synthetic methods to yield these clusters have been developed.

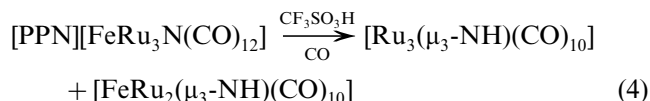
2.2.1. Use of nitrosyl compounds

The mixed-metal clusters that contain imido ligands can be prepared by the coupling reaction between the mononuclear complex and the cluster complex [68–72] or two mononuclear complexes [73–75]. Usually, one of the starting materials contains the nitrogen functionalities, which can be transformed into imido ligands directly via the coupling reaction. Wong et al. recently reported the imido-capped ruthenium–cobalt mixed-metal clusters were prepared from the reaction between [Ru₃(μ-H)₂(μ₃-NOMe)(CO)₉] and [Cp*Co(CO)₂] (Cp* = η⁵-C₅Me₅) (Scheme 15) [68,69].

According to the relevant reactions that were observed in a homometallic system containing the NO ligand, the mixed-metal cluster containing the μ₃-NH ligand can be obtained from the reduction of its μ₃-NO containing nitrosyl analogues. This ligand transformation is supported by the isolation of cluster [MnFe₂(μ₂-CO)₂(μ₂-NO)(μ₃-NH)]⁺ directly from the reaction of [MnFe₂(μ₂-CO)₂(μ₂-NO)(μ₃-NO)] either with HBF₄ or a variety of oxidants (Ag⁺, NO⁺, NO₂⁺, Br₂ and I₂) [76].

2.2.2. Use of nitrido mixed-metal clusters

The protonation (Eq. (4)) or thermolysis (Scheme 16) of mixed-metal clusters containing (μ₄-N) nitrido compound are promising routes for imido cluster preparation [66,77]. However, the nature of product is difficult to predict as protonation on the metal edge is always a competition.



2.2.3. Use of imido metal clusters

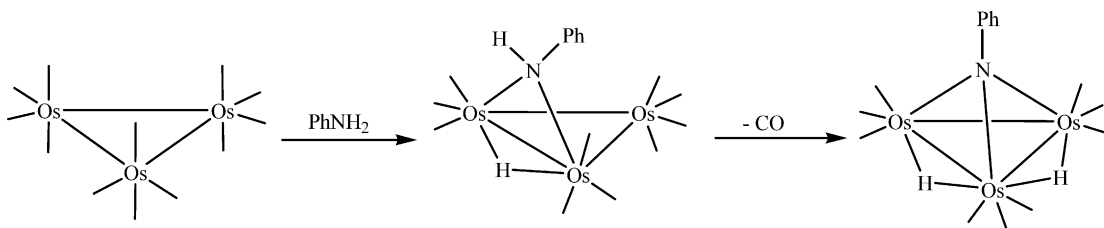
The mixed-metal clusters that contain imido ligands can be prepared by the direct reaction of a homometallic imido cluster with another metal compound [78–80]. The imido-capped mixed-metal cluster [Cp*W(O)(μ-O)Ru₃(μ₃-NPh)(CCPh)(CO)₈] has been obtained from the reaction of [Ru₃(μ₃-NPh)(μ₃-CO)(CO)₉] with [Cp*W(O)₂(CCR)] [78]. Heating of this imido cluster with [Ru₃(CO)₁₂] in toluene at reflux gave [Cp*W(O)(μ-O)Ru₄(μ₄-NPh)(CCPh)(μ-CO)(CO)₉] in high yield (Scheme 17).

3. Structural properties

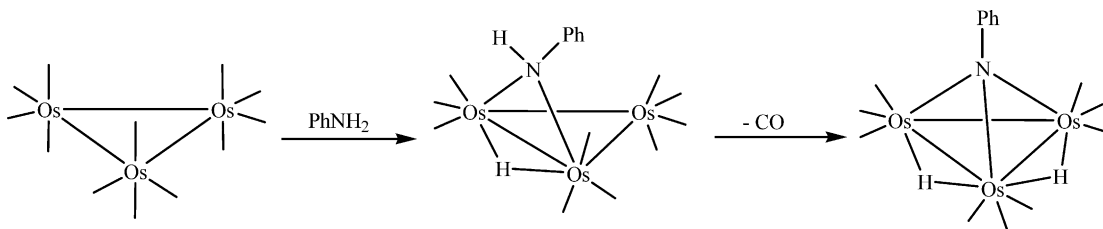
In the last few decades, numerous low valent transition metal clusters that contain imido ligands have been prepared, and their molecular structures have been established by X-ray crystallography. Several common structural features of these reported clusters will be discussed.

3.1. d⁸ Transition metal cluster series (Fe, Ru and Os)

Detailed structural studies have been conducted for the d⁸ transition metal carbonyl clusters that contain imido ligands, especially the trinuclear carbonyl clusters that are triply capped with imido ligands. The triangular trimetal core is either monocapped or bicapped with ligands, see Fig. 1. The bicapped species may contain other capping ligands, (μ₃-X) (X = CO [13], PR [81], and



Scheme 9.



Scheme 10.

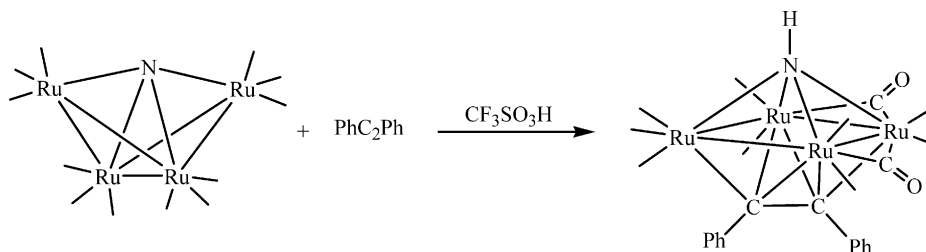
S[82]) as well as the capping imido ligands. The variation in the electron donating ability of these capping ligands may lead to marked changes in cluster geometry. The trinuclear carbonyl clusters $[\text{M}_3(\mu_3\text{-NR})(\text{CO})_9(\mu_3\text{-X})]$ that are bicapped with four-electron donors, such as imido and phosphorus ligands, lead to a metal-metal bond cleavage as expected from the effective atomic number (EAN) rules. However, the trigonal bipyramid geometry that is observed in the closed triangular bicapped species remains nearly unchanged, as the capping ligands significantly enhance the rigidity of these structures. Examples of monocapped species, such as $[\text{M}_3(\mu\text{-H})_2(\text{CO})_9(\mu_3\text{-NR})]$ ($\text{M} = \text{Fe}$ [45], Ru [83] and Os [30]), are relatively rare when compared to the bicapped species. The metal hydrides, serving as one-electron donors, are usually involved in these clusters. The hydride-bridged metal-metal bond is significantly elongated.

The formation of the quadruply capped imido metal cluster is rather rare when compared to the triply capped system. The only examples of iron clusters containing $\mu_4\text{-NR}$ imido ligands that have been established by X-ray analysis are $[\text{Fe}_4(\mu_4\text{-NEt})(\mu_4\text{-}\eta^2\text{-NOEt})(\mu\text{-CO})_3(\text{CO})_8]$ [84] and $[\text{Fe}_4(\mu_4\text{-NEt})_2(\mu\text{-CO})(\text{CO})_{10}]$ [37], the schematic diagrams of which are depicted in Fig. 2. Four iron atoms define a distorted square planar geometry and are quadruply bicapped with ligands ($\mu_4\text{-}\eta^2\text{-NOEt}$ and $\mu_4\text{-NEt}$) on both sides. More examples of quadruply capped imido ruthenium carbonyl clusters have been established by Wong et al. in recent years [51–55,69]. It is noteworthy that the isolation of the tetraruthenium clusters which contain $\mu_4\text{-NR}$ ($\text{R} = \text{H}$, Ph , $\text{C}(\text{O})\text{OMe}$) imido ligands usually involve a trapping agent. The alkynes $[\text{RC}_2\text{R}']$ ($\text{R}/\text{R}' = \text{Ph}$, Tol , H , COOMe , C_2Ph) are most commonly used as the stabilizing agents, and display a great variety of

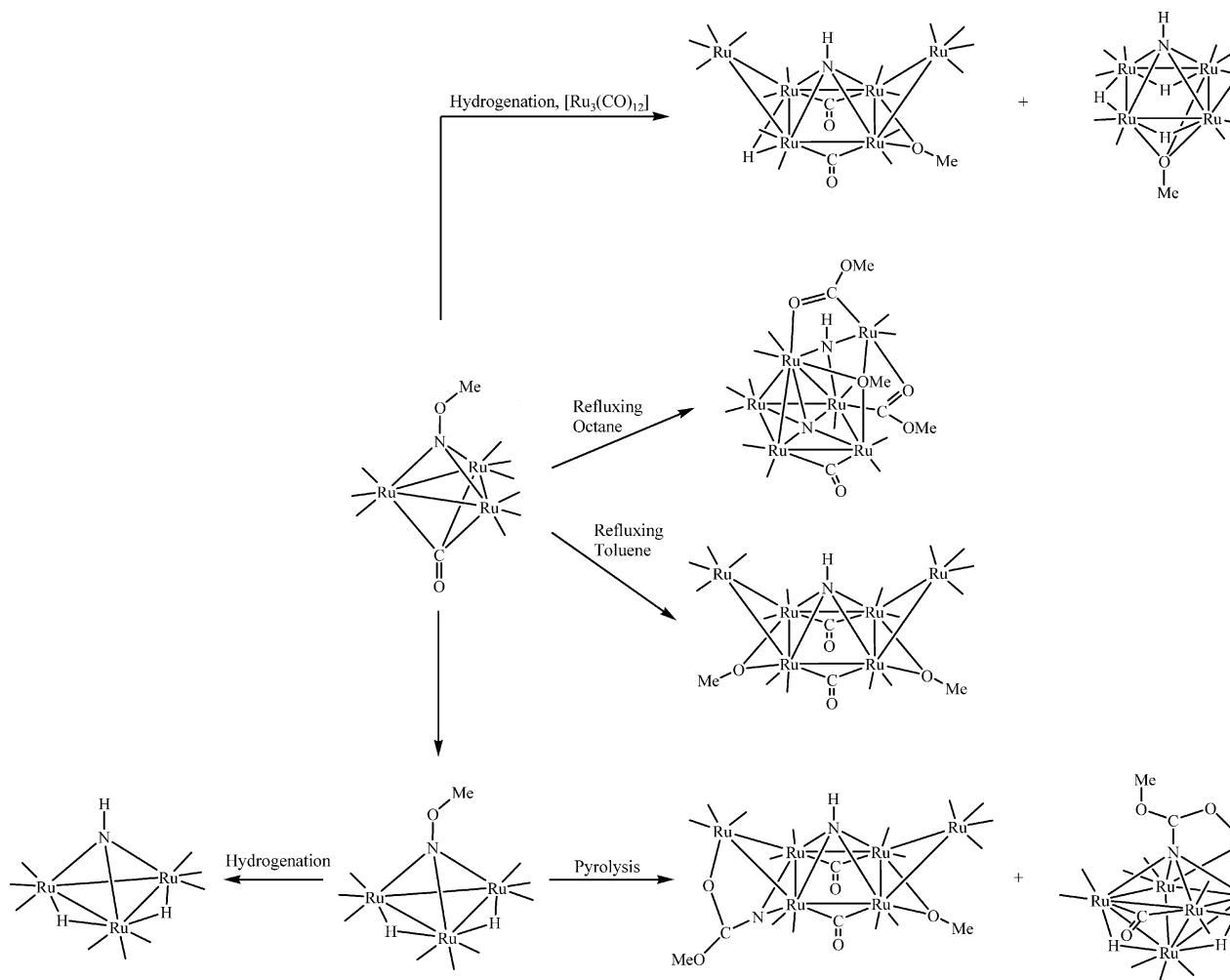
interactions that result from the possibility of varying the substituents, and hence the polarity of the triple bond. The acetylene ligands act as various electron donors (between 1 and 5) in polynuclear cluster systems, which effectively stabilize the molecular configuration. Similar stabilized structures have been observed in pentaruthenium systems, such as $[\text{Ru}_5(\text{CO})_{13}(\mu\text{-CO})(\mu_4\text{-NH})(\mu_4\text{-}\eta^2\text{-HC}_2\text{Ph})]$ [55], $[\text{Ru}_5(\mu\text{-H})(\text{CO})_9(\mu\text{-CO})_3(\eta^5\text{-Cp}^*)(\mu_4\text{-NH})]$ [69], and $[\text{Ru}_5(\mu\text{-H})_3(\text{CO})_{13}(\mu_4\text{-NH})(\mu_3\text{-OMe})]$ [53]. A schematic diagram of $[\text{Ru}_5(\mu\text{-H})(\text{CO})_9(\mu\text{-CO})_3(\eta^5\text{-Cp}^*)(\mu_4\text{-NH})]$ is shown in Fig. 3. The square pyramid metal framework is formed with five ruthenium atoms, and the imido ligand is quadruply capping on the square plane. This structure is analogous to the bicapped tetraruthenium carbonyl clusters $[\text{Ru}_4(\text{CO})_9(\mu\text{-CO})_2(\mu_4\text{-NH})(\mu_4\text{-}\eta^2\text{-RC}_2\text{R}')]_2$, and is supposed to have a stabilizing effect that is similar to those observed in tetranuclear species.

Clusters with monocapped $\mu_4\text{-NR}$ imido ligands have been observed in hexaruthenium systems [53]. The ruthenium atoms are arranged in a boat shape, as shown in Fig. 4, where the quadruply bridged imido ligand is situated on the central square plane. This suggests that the $\mu_4\text{-NR}$ group is more stabilized in this boat-shaped cluster than in the square planar tetraruthenium cluster. There is no isolation of the osmium carbonyl cluster that contains the $\mu_4\text{-NR}$ imido ligand. However, the formation of the $\mu_4\text{-NR}$ imido tetraosmium cluster is believed to be possible with the aid of a suitable stabilizing agent.

The metal–nitrogen ($\text{M}-\text{N}$) and metal–metal ($\text{M}-\text{M}$) bond distances of these d^8 transition metal clusters are summarized in Figs. 5 and 6, respectively. $\text{M}-\text{NR}$ bond distances are found to increase from $\text{Fe}-\text{N}$ to $\text{Ru}-\text{N}$ and $\text{Os}-\text{N}$. Furthermore, the $\text{M}-\text{M}$ bond distances in the opened triangular structures are shown to be



Scheme 11.

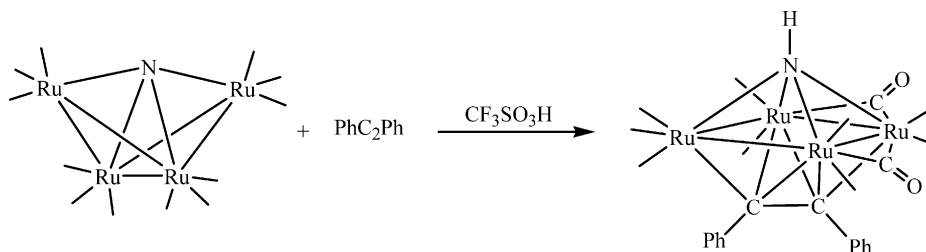


Scheme 12.

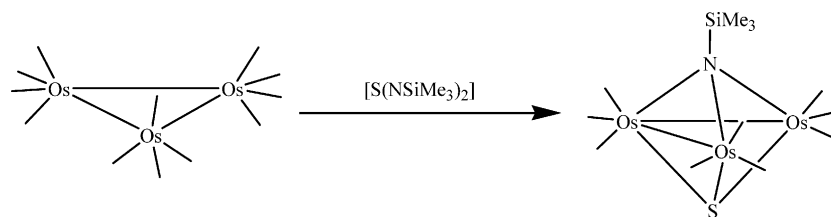
shortened when compared to the values that have been observed in the closed triangular structure, while the overall cluster geometry is more or less the same. The $M \cdots M$ bond distances of the opened triangular species are usually over 3 Å, which also increases down the group. In contrast, the $M-N$ bond distances in the opened triangular structure are longer than the equivalent value that is observed in the closed triangular structure. It is noteworthy that the μ_3 and μ_4 -capped imido clusters show a considerable difference in the $M-N$ bond distances. However, their $M-M$ bond lengths are comparable.

3.2. d^9 Transition metal cluster series (Co and Rh)

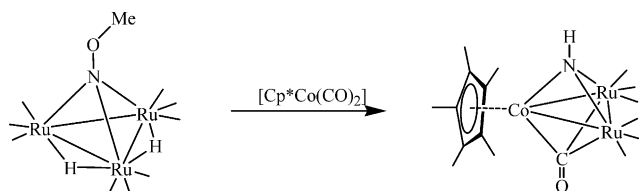
Structural investigation has also been carried out on the d^9 transition metal clusters that contain capping imido ligands, especially the cobalt system. Numerous structures of the imido capped tricobalt clusters $[Co_3(\mu_3-Y)(\mu_3-X)(\eta^5-C_5H_5-xMe_x)_3]$ ($x = 0, 1, 5$; $X = CO, NO$; $Y = NSiMe_3, NC(O)NH_2, NH$) have been reported by Dahl and coworkers [28]. As shown in Fig. 7, all of these clusters are triply bicapped with imido groups and other electron-donating ligands ($-NO$, $-CO$ and S), which have trinuclear structures that are similar to those



Scheme 13.



Scheme 14.



Scheme 15.

observed in d^8 transition metal species. However, no opened triangular clusters have been observed in the cobalt complexes. These structures are coordinated with cyclopentadiene ligands, which serve as five-electron donors, and the structures are complied with the EAN rule. The cluster $[Co_6(\mu_4-NPh)(\mu-NPh)_6(PPh_2Et)_2]$ [85] is the only example of a cobalt cluster that contains a quadruply bridged imido ligand. As shown in Fig. 8, the cobalt atoms are arranged in a plane, which is different from the boat-shaped geometry that is observed in the hexaruthenium imido cluster, with the μ_4-NPh ligand situated on the central square plane. The Co–N [1.786–1.934 Å] and Co–Co [2.356–2.61 Å] bond distances of these clusters are comparable to those that have been observed in imido-capped iron carbonyl clusters. Furthermore, the capping imido ligands have also been found to be good stabilizing ligands in high nuclearity cobalt clusters such as $[Co_8(\mu_3-NPh)_6(\mu-NPh)_3(PPh_3)_2]$ [85] and $[Co_{11}(\mu_3-NPh)_6(\mu-NPh)_6(PPh_3)_3]$ [86].

Examples of rhodium imido clusters are rare and limited to the $\mu_3-NC_6H_4Me$ imido ligand [87–90]. The hexarhodium imido cluster $[Rh_6(\mu_3-NC_6H_4Me)(CO)_{12}]$ [87] has a metal core architecture that is analogous with cobalt cluster $[Co_6(\mu_4-NPh)(\mu-NPh)_6(PPh_2Et)_2]$, which consists of two open triangular trirhodium metal

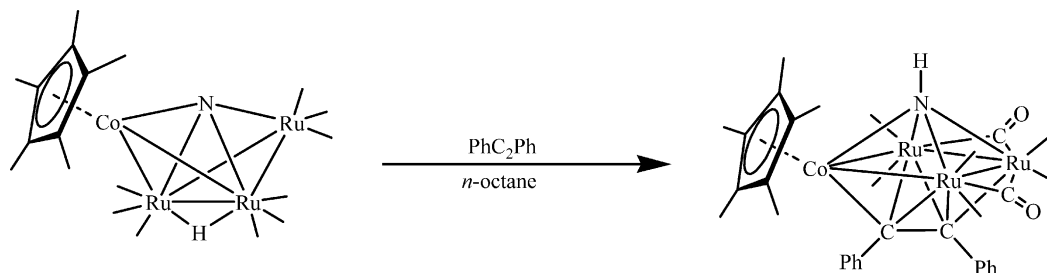
clusters (Fig. 9). There are four imido ligands triply capping on the triangular metal planes, and the non-bonded Rh··Rh distance is 3.113 Å.

3.3. Other transition metal clusters

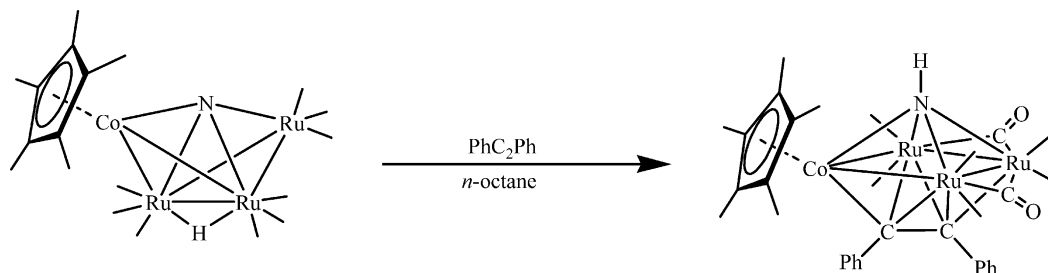
Apart from the aforementioned examples, the triply or quadruply bridging imido ligands have also been observed in other low valent transition metal clusters, such as gold [56–61], nickel [62–64,86], copper [86,91–93], chromium [94,95], rhenium [96,97], manganese [49], and tungsten [98]. Most of these clusters are trinuclear ionic species with triply capping imido ligands, and have similar structures to those which have been observed in d^8 and d^9 transition metal series. In addition, the capping NR imido moieties are commonly observed in some high nuclearity transition metals clusters, such as copper and nickel. The metal–nitrogen and metal–metal bond distances of these clusters are summarized in Figs. 10 and 11, respectively. The M–N bond distance of the third row transition metal clusters are notably lengthened when compared to the values which have been observed in the first row metal clusters. Nevertheless, the variation in metal–metal bond distances is not significant down the row. However, it is noteworthy that the Au–Au bond [2.942–3.281 Å] distances are exceptionally elongated, which is probably due to the weak intramolecular interactions between the gold(I) centers (Fig. 12). The stability of these clusters varies with the donor strength of the phosphine ligand.

3.4. Heterometallic transition metal clusters

Numerous structures of the imido-capped transition mixed-metal clusters have been established and studied. Most of these mixed-metal clusters consist of d^8 and d^9



Scheme 16.



Scheme 17.

transition metals, and they exhibit similar molecular configurations as their homometallic analogous. The typical examples are ruthenium–cobalt and ruthenium–molybdenum mixed-metal imido clusters, as shown in Fig. 13, where the ruthenium fragment $[\text{Ru}(\text{CO})_3]$ is substituted with $[\text{Co}(\text{Cp})]$ [69] and $[\text{Mo}(\text{CO})_2(\text{Cp})]$ [70] respectively. The exchange of metal fragments may lead to variation in metal-metal bond distances accompanied by a slight distortion of cluster geometry. In addition, there are examples of the ligand being substituted by its isolobal metal fragment. As shown in Fig. 14, the structure of mixed-metal cluster $[\text{Ru}_3(\mu_3\text{-NPh})(\text{CO})_9(\text{AuPPh}_3)_2]$ [99] is comparable to $[\text{Ru}_3(\mu_3\text{-H})(\mu_3\text{-NPh})(\text{CO})_9]$, although the $[\text{AuPPh}_3]$ is not strictly isolobal with the hydride ligand in this case.

4. NMR spectroscopic properties of (μ_3 or μ_4 -NH) imido ligands

The ^1H - and ^{15}N -NMR studies of the imido ligands are significant partly because they provide strong evidence to support the existence of imido protons, which cannot be located easily by X-ray crystallographic studies, and more importantly because these signals provide information about the electronic environment of the imido nitrogen and hydrogen atoms.

4.1. ^1H -NMR spectroscopy

The ^1H -NMR signals of the μ_3 - and μ_4 -NH imido ligands of low valent transition metal clusters are shown

in the Tables 1 and 2, respectively. As shown in Fig. 15, the μ_3 -NH signals of these clusters are observed in a broad NMR range from $\delta = -0.33$ to $+24.92$. The most deshielded imido proton NMR signals are observed in the cationic clusters $[\text{Mn}_3(\eta^5\text{-C}_5\text{H}_4\text{Me})_3(\mu_3\text{-NO})_3(\mu_3\text{-NH})]^+$ and $[\text{MnFe}_2(\eta^5\text{-Cp}^*)(\eta^5\text{-Cp})_2(\mu_2\text{-CO})_2(\mu_2\text{-NO})(\mu_3\text{-NH})]^+$. Among the neutral clusters, $[\text{Ru}_6(\text{CO})_{13}(\mu\text{-CO})(\mu_3\text{-NH})(\mu_5\text{-N})(\mu_3\text{-OMe})\{\mu_2\text{-}\eta^2\text{-C}(\text{O})\text{OMe}\}_2]$ has the most shielded imido proton signal, which is attributed to the presence of the electron donating groups such as $\mu_5\text{-N}$ and $\mu_3\text{-OMe}$ ligands. Comparing the NH signals of clusters $[\text{Fe}_3(\text{CO})_9(\mu_3\text{-NCH}_2\text{CH}_3)(\mu_3\text{-NH})]$, $[\text{Fe}_3(\text{CO})_9(\mu_3\text{-NH})_2]$ and $[\text{Fe}_3(\text{CO})_9(\mu_3\text{-CO})(\mu_3\text{-NH})]$, we observed that the chemical shift of the NH ligand is directly correlated to the electron-donating ability of the capping ligands. The more electron donating capping ligand pushes the imido proton signal more upfield ($\mu_3\text{-CO} < \mu_3\text{-NH} < \mu_3\text{-NCH}_2\text{CH}_3$).

In addition, the cluster $[\text{Ru}_3(\text{CO})_9(\mu_3\text{-CO})(\mu_3\text{-NH})]$ ($\delta = 5.70$) shows a significant shielded imido proton signal when compared to its iron analogue $[\text{Fe}_3(\text{CO})_9(\mu_3\text{-CO})(\mu_3\text{-NH})]$ ($\delta = 9.50$), and an intermediate chemical shift of NH ($\delta = 6.50$) is observed in their bimetallic analogue $[\text{Ru}_2\text{Fe}(\text{CO})_9(\mu_3\text{-CO})(\mu_3\text{-NH})]$. As the coordination ligands and cluster geometry of these three clusters are exactly the same, the significant differences in chemical shift are attributed to the effect of the transition metal. This proposal is further supported by the marked difference ($\Delta\delta = 1.76$ ppm) in NH signal between the clusters $[\text{Ru}_3(\text{CO})_9(\mu_3\text{-CO})(\mu_3\text{-NH})]$ and $[\text{Ru}_2\text{Co}(\text{CO})_6(\mu_3\text{-CO})(\eta^5\text{-Cp}^*)(\mu_3\text{-NH})]$. Further-

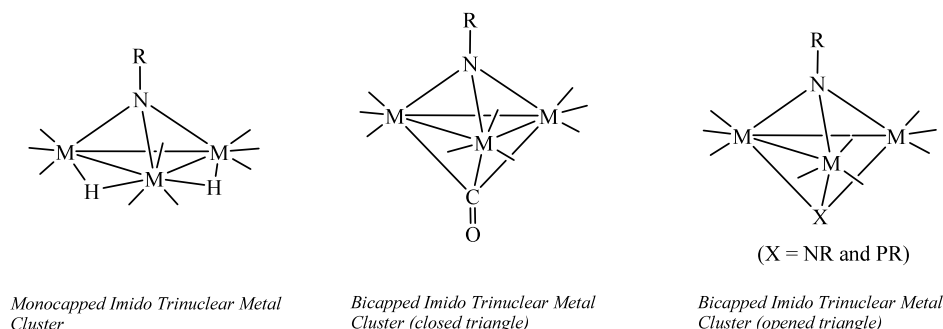


Fig. 1. A schematic diagram of mono and bicapped imido trinuclear metal clusters.

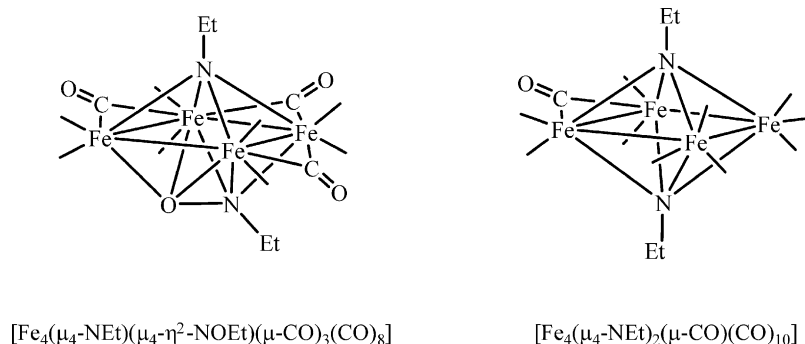


Fig. 2. A schematic diagram of clusters $[\text{Fe}_4(\mu_4\text{-NEt})(\mu_4\text{-}\eta^2\text{-NOEt})(\mu\text{-CO})_3(\text{CO})_8]$ and $[\text{Fe}_4(\mu_4\text{-NEt})_2(\mu\text{-CO})(\text{CO})_{10}]$.

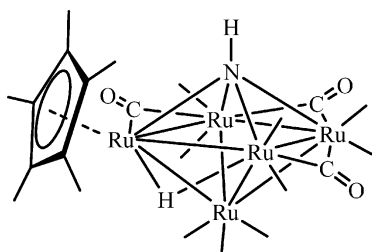
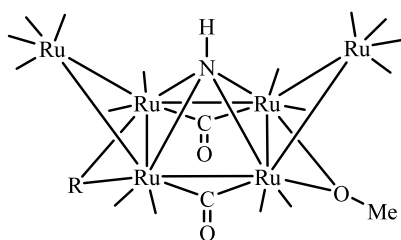


Fig. 3. A schematic diagram of cluster $[\text{Ru}_5(\mu\text{-H})(\text{CO})_9(\mu\text{-CO})_3(\eta^5\text{-Cp}^*)(\mu_4\text{-NH})]$.



R = OMe, NCO, NC(O)OMe and H

Fig. 4. A schematic diagram of hexaruthenium metal clusters containing $\mu_4\text{-NH}$ imido ligand.

more, the NH ligands in the tricobalt clusters $[\text{Co}_3(\eta^5\text{-Cp}^*)_2(\eta^5\text{-C}_5\text{H}_4\text{Me})(\mu_3\text{-CO})(\mu_3\text{-NH})]$ and $[\text{Co}_3(\eta^5\text{-Cp}^*)(\eta^5\text{-C}_5\text{H}_4\text{Me})_2(\mu_3\text{-CO})(\mu_3\text{-NH})]$ are highly deshielded when compared to the structurally similar ruthenium complexes. The metal effect on the imido proton NMR signal appears to be significant.

As shown in Fig. 16, most examples of $\mu_4\text{-NH}$ imido ligands are observed in ruthenium metal clusters, which exhibit imido proton NMR signals within the range of δ 1.87–6.28. The only example of a $\mu_4\text{-NH}$ ligand in a bimetallic cluster $[\text{Ru}_3\text{Co}(\text{CO})_6(\mu\text{-CO})_2(\eta^5\text{-Cp}^*)(\mu_4\text{-NH})(\mu_4\text{-}\eta^2\text{-PhC}_2\text{Ph})]$ shows a positive shift ($\Delta\delta = 0.89$ ppm) in the NH proton signal when compared to its homometallic analogue $[\text{Ru}_4(\text{CO})_9(\mu\text{-CO})_2(\mu_4\text{-NH})(\mu_4\text{-}\eta^2\text{-PhC}_2\text{Ph})]$. In addition, the more electron donating $\mu_3\text{-PN}^i\text{Pr}_2$ ligand makes the imido proton signal of $[\text{Ru}_5(\text{CO})_{10}(\mu\text{-CO})_2(\mu_3\text{-CO})(\mu_4\text{-NH})(\mu_3\text{-PN}^i\text{Pr}_2)]$ more

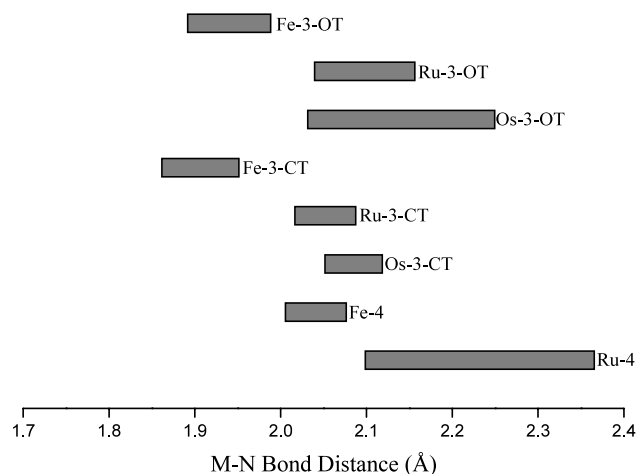


Fig. 5. Ranges of M–N bond distances of imido-capped d^8 transition metal clusters (OT = opened triangle; CT = closed triangle; 3 = μ_3 ; 4 = μ_4).

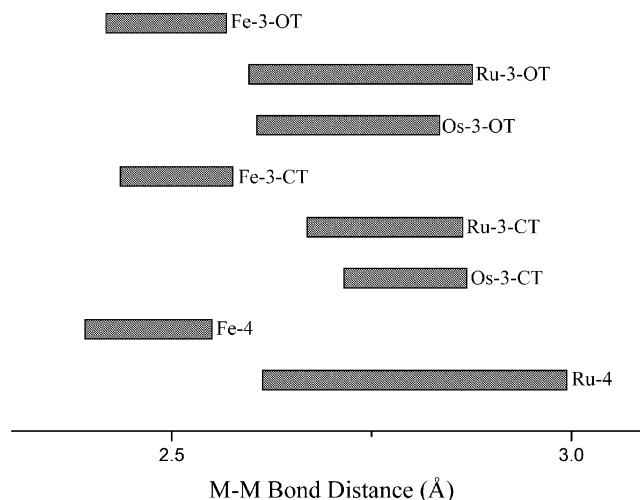


Fig. 6. Ranges of M–M bond distances of imido-capped d^8 transition metal clusters (OT = opened triangle; CT = closed triangle; 3 = μ_3 ; 4 = μ_4).

shielded when compared to the structurally similar cluster $[\text{Ru}_5(\mu\text{-H})(\text{CO})_9(\mu\text{-CO})_3(\eta^5\text{-Cp}^*)(\mu_4\text{-NH})]$. Apart from the metal and ligand effect that was

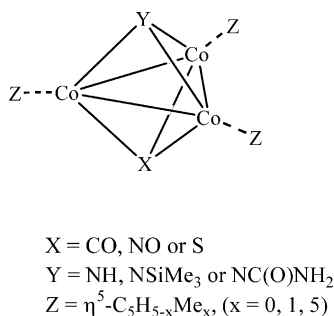


Fig. 7. A schematic diagram of cluster $[\text{Co}_3(\mu_3\text{-Y})(\mu_3\text{-X})(\eta^5\text{-C}_5\text{H}_{5-x}\text{Me}_x)_3]$.

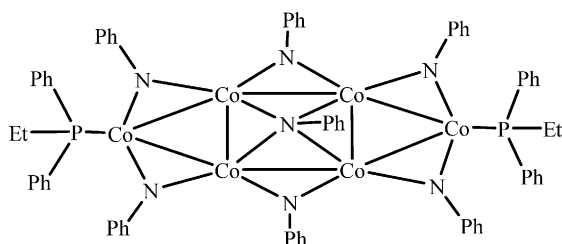


Fig. 8. A schematic diagram of cluster $[\text{Co}_6(\mu_4\text{-NPh})(\mu\text{-NPh})_6(\text{PPh}_2\text{Et})_2]$.

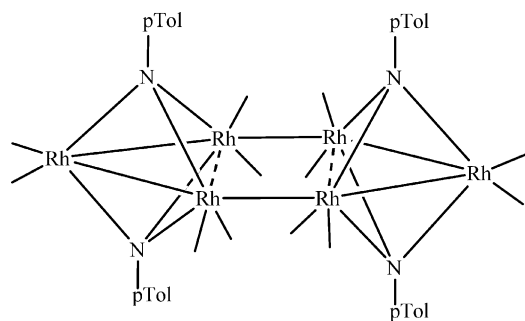


Fig. 9. A schematic diagram of cluster $[\text{Rh}_6(\mu_3\text{-NC}_6\text{H}_4\text{Me})_4(\text{CO})_{12}]$.

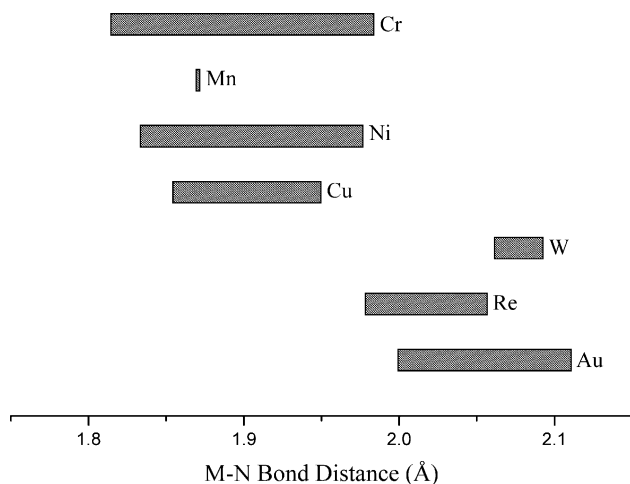


Fig. 10. Ranges of M–N bond distances of selected imido-capped transition metal clusters.

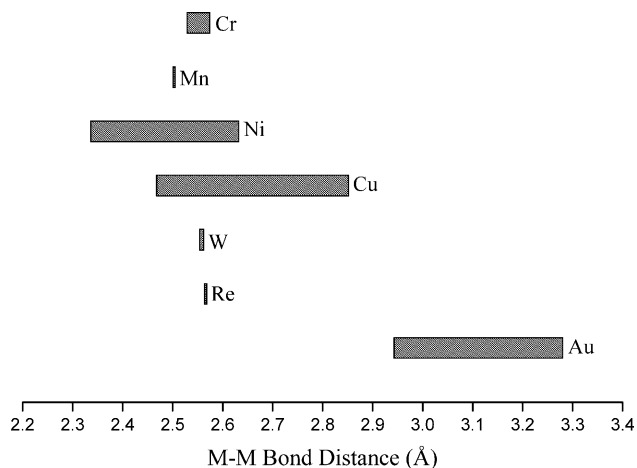


Fig. 11. Ranges of M–M bond distances of selected imido-capped transition metal clusters.

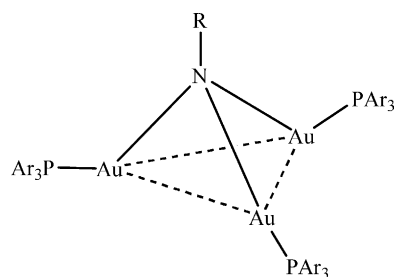


Fig. 12. A schematic diagram of gold metal cluster containing triply bridging imido ligands.

mentioned for the $\mu_3\text{-NH}$ system, this shows that the imido proton signal is also associated with the cluster nuclearity. Comparing the imido proton signals of $[\text{Ru}_4(\text{CO})_9(\mu\text{-CO})_2(\mu_4\text{-NH})(\mu_4\text{-}\eta^2\text{-PhC}_2\text{Ph})]$ and $[\text{Ru}_5(\text{CO})_{13}(\mu\text{-CO})(\mu_4\text{-NH})(\mu_4\text{-}\eta^2\text{-HC}_2\text{Ph})]$, it seems that the increasing in cluster nuclearity shifts the signal to be more downfield. This is further supported by the relative deshielded NH signals within the range of δ 5.55–6.18 that are observed in hexaruthenium complexes.

4.2. ^{15}N -NMR spectroscopy

The chemical shift in ^{15}N -NMR spectroscopy is sensitive to local geometry, and it is a useful tool in characterizing imido clusters. However, only a few imido clusters have been investigated by ^{15}N -NMR spectroscopy, and most of them are ruthenium complexes (Fig. 17). The ^{15}N -NMR data of several imido-capped transition metal clusters are listed in Table 3. The ^{15}N -NMR signal of the $\mu_3\text{-NH}$ nitrogen atom of the heterometallic clusters are significantly downfield when compared to that of triruthenium $\mu_3\text{-NH}$ cluster $[\text{Ru}_3(\mu_3\text{-CO})(\text{CO})_9(\mu_3\text{-NH})]$. This can be attributed to the metal effect that has been observed in ^1H -NMR signal. However, all of these clusters feature a coupling

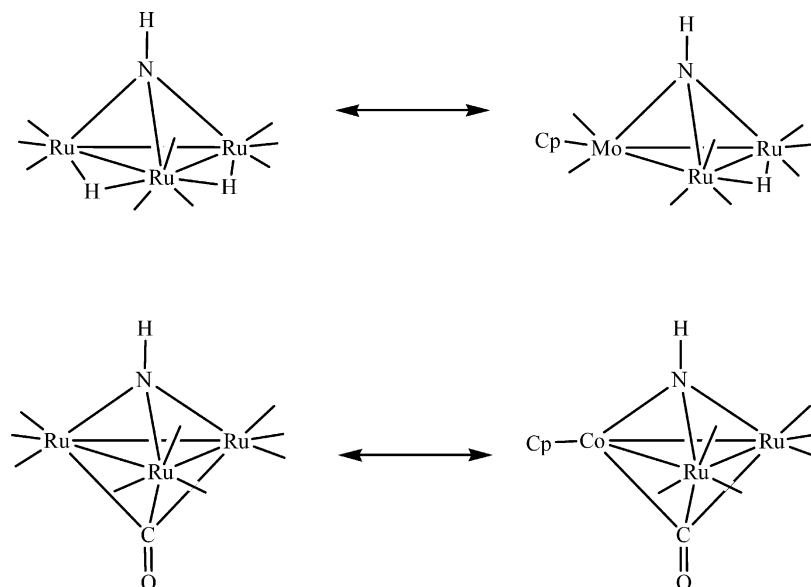


Fig. 13. Comparison between imido (mono- and bicapped) ruthenium metal clusters and their bimetallic analogues.

constant that is around 77 Hz, which is characteristic of a direct N–H bond. The ^{15}N –H coupling can be converted to the ^{14}N –H coupling by the equation $J(^{14}\text{N}\text{--H}) = -0.713 \times J(^{15}\text{N}\text{--H})$, in which -0.713 comes from γ_{14}/γ_{15} [100]. Nitrogen J couplings, which are dependent on the geometry [101] and hybridization [102] of the nitrogen, are particularly valuable in structural determination because of their sensitivity to the presence and orientation of a lone pair on the nitrogen.

Hence, the chemical shifts of μ_4 -NH nitrogen atoms are more shielded than the values that are observed in μ_3 -NH clusters. This effect may correspond to the diamagnetic ‘ring current’ in the unsaturated square planar clusters. Unsurprisingly, the nitrogen resonance of $[\text{Ru}_3\text{Co}(\text{CO})_6(\mu\text{-CO})_2(\eta^5\text{-Cp}^*)(\mu_4\text{-NH})(\mu_4\text{-}\eta^2\text{-PhC}_2\text{Ph})]$ shows a positive shift ($\Delta\delta = 22.6$ ppm) when compared to $[\text{Ru}_4(\text{CO})_9(\mu\text{-CO})_2(\mu_4\text{-NH})(\mu_4\text{-}\eta^2\text{-PhC}_2\text{Ph})]$. Moreover, the ^{15}N resonance of $[\text{Ru}_5(\mu\text{-H})(\text{CO})_9(\mu\text{-CO})_3(\eta^5\text{-Cp}^*)(\mu_4\text{-NH})]$ is significantly downfield when compared to that of $[\text{Ru}_4(\text{CO})_9(\mu\text{-CO})_2(\mu_4\text{-NH})(\mu_4\text{-}\eta^2\text{-PhC}_2\text{Ph})]$, which conforms to the trend of increasing magnitude with increasing nuclearity around the imido nitrogen. Thus, the greater the

number of metal atoms that are bonded to the nitrogen moiety, the more deshielded is the nitrogen resonance. A similar trend has been observed in the μ_3 -NH system. It is also noteworthy that the coupling constants for direct ^{15}N – ^1H interactions in the μ_4 -NH moieties are slightly smaller than those for the μ_3 -NH groups. These characteristic values provide useful information for ascertaining whether the imido ligand is bound to three or four metal centers.

5. Reactivities

5.1. Reactions toward alkynes

Alkynes are known to be good stabilizing agents for trapping quadruply capped imido clusters; consequently, the reactions between imido clusters and alkynes have been investigated in detail [103–109]. In the 1990s, Geoffroy et al. reported on the reactions of μ_3 -NPh capped trinuclear metal clusters with alkynes ($\text{RC}_2\text{R}'$) in refluxing hexane to form binuclear metallapyrrolinone complexes $[\text{M}_2\{\mu_2\text{-}\eta^3\text{-RC=CR}'\text{C}(\text{O})\text{NPh}\}(\text{CO})_6]$ ($\text{M} = \text{Fe}$ and Ru) and tetranuclear derivatives

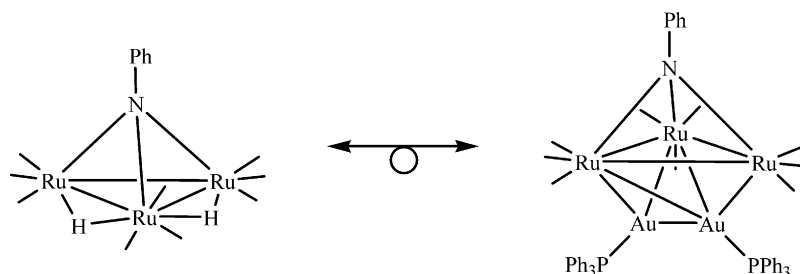


Fig. 14. Comparison between the isolobal clusters $[\text{Ru}_3(\mu\text{-H})_2(\mu_3\text{-NPh})(\text{CO})_9]$ and $[\text{Ru}_3(\text{AuPPh}_3)_2(\mu_3\text{-NPh})(\text{CO})_9]$.

Table 1
¹H-NMR data of transition metal clusters containing μ₃-NH ligand

| Formula | Chemical shift of (μ ₃ -NH) ligand | Ref. |
|--------------------------------------------------------------------------------------------------------------------------------------------------------------------------------------------------------|-----------------------------------------------|-------|
| Fe ₃ (CO) ₉ (μ ₃ -NCH ₂ CH ₃)(μ ₃ -NH) | 3.77 | [46] |
| Fe ₃ (CO) ₉ (μ ₃ -NH) ₂ | 5.30 | [46] |
| Fe ₃ (CO) ₉ (μ ₃ -CO)(μ ₃ -NH) | 9.50 | [47] |
| Ru ₃ (CO) ₉ (μ ₃ -CO)(μ ₃ -NH) | 5.70 | [77] |
| Ru ₃ (μ-H) ₂ (CO) ₉ (μ ₃ -NH) | 6.33 | [53] |
| Ru ₆ (CO) ₁₃ (μ-CO)(μ ₃ -NH)(μ ₅ -N)(μ ₃ -OMe){μ ₂ -η ² -C(O)OMe} ₂ | −0.33 | [52] |
| Fe ₂ Mo(CO) ₆ (μ ₂ -CO)(η ⁵ -C ₅ H ₅)(μ ₃ -NH)(μ ₂ -NO) | 1.44 | [74] |
| Ru ₂ Mo(μ-H)(CO) ₈ (η ⁵ -C ₅ H ₅)(μ ₃ -NH) | 6.05 | [70] |
| Ru ₂ Fe(CO) ₉ (μ ₃ -CO)(μ ₃ -NH) | 6.50 | [77] |
| Ru ₂ Fe(CO) ₉ (μ ₃ -NH){P(OMe) ₃ } | 6.70 | [77] |
| Ru ₃ Co ₂ (CO) ₇ (μ ₃ -CO)(η ⁵ -Cp*) ₂ (μ ₃ -NH){μ ₄ -η ⁸ -C ₆ H ₄ C(H)C(Ph)} | 4.94 | [68] |
| Ru ₂ Co(CO) ₆ (μ ₃ -CO)(η ⁵ -Cp*)(μ ₃ -NH) | 7.46 | [69] |
| Os ₄ (μ-H) ₂ (CO) ₁₂ (μ ₃ -NH) | 9.10 | [42] |
| W ₃ (μ ₃ -NH)(O [−] Pr) ₁₀ | 9.87 | [96] |
| Co ₃ (η ⁵ -Cp*) ₂ (η ⁵ -C ₅ H ₄ Me)(μ ₃ -CO)(μ ₃ -NH) | 12.09 | [117] |
| Co ₃ (η ⁵ -Cp*)(η ⁵ -C ₅ H ₄ Me) ₂ (μ ₃ -CO)(μ ₃ -NH) | 12.86 | [117] |
| [Mn ₃ (η ⁵ -C ₅ H ₄ Me) ₃ (μ ₃ -NO) ₃ (μ ₃ -NH)] ⁺ | 21.95 | [49] |
| [MnFe ₂ (η ⁵ -Cp*)(η ⁵ -Cp*) ₂ (μ ₂ -CO) ₂ (μ ₂ -NO)(μ ₃ -NH)] ⁺ | 24.92 | [76] |

Table 2
¹H-NMR data of transition metal clusters containing μ₄-NH ligand

| Formula | Chemical shift of (μ ₄ -NH) ligand | Ref. |
|--------------------------------------------------------------------------------------------------------------------------------------------------------|-----------------------------------------------|------|
| Ru ₄ (CO) ₉ (μ-CO) ₂ (μ ₄ -NH)(μ ₄ -η ² -PhC ₂ Ph) | 1.87 | [55] |
| Ru ₄ (CO) ₉ (μ-CO) ₂ (μ ₄ -NH)(μ ₄ -η ² -HC ₂ Tol) | 1.96 | [54] |
| Ru ₅ (CO) ₁₀ (μ-CO) ₂ (μ ₃ -CO)(μ ₄ -NH)(μ ₃ -PN ⁱ Pr ₂) | 3.22 | [50] |
| Ru ₅ (CO) ₁₃ (μ-CO)(μ ₄ -NH)(μ ₄ -η ² -HC ₂ Ph) | 3.72 | [55] |
| Ru ₅ (μ-H) ₃ (CO) ₁₃ (μ ₄ -NH)(μ ₃ -OMe) | 5.00 | [53] |
| Ru ₅ (μ-H)(CO) ₉ (μ-CO) ₃ (η ⁵ -Cp*)(μ ₄ -NH) | 6.28 | [69] |
| Ru ₆ (CO) ₁₅ (μ-CO) ₂ (μ ₄ -NH)(μ-OMe){μ ₃ -η ² -N(H)C(O)OMe} | 5.55 | [51] |
| Ru ₆ (CO) ₁₆ (μ-CO) ₂ (μ ₄ -NH)(μ-OMe)(μ-NCO) | 5.70 | [51] |
| Ru ₆ (CO) ₁₆ (μ-CO) ₂ (μ ₄ -NH)(μ-OMe) ₂ | 5.75 | [53] |
| Ru ₆ (μ-H)(CO) ₁₆ (μ-CO) ₂ (μ ₄ -NH)(μ-OMe) | 5.92 | [53] |
| Ru ₆ (μ-H)(CO) ₁₆ (μ-CO)(μ ₄ -NH){μ ₃ -η ² -C(O)OMe} | 6.18 | [53] |
| Ru ₃ Co(CO) ₆ (μ-CO) ₂ (η ⁵ -Cp*)(μ ₄ -NH)(μ ₄ -η ² -PhC ₂ Ph) | 2.76 | [69] |

(Scheme 18) [103,104]. The diversity of products in these reactions is surprising, given that there is a total lack of correspondence between the reactions of alkynes with analogous imido and phosphinidene clusters. The formation of metallapyrrolinone products from imido complexes reflect the fact that the RN–C(O) bond is stronger than the RP–C(O) bond.

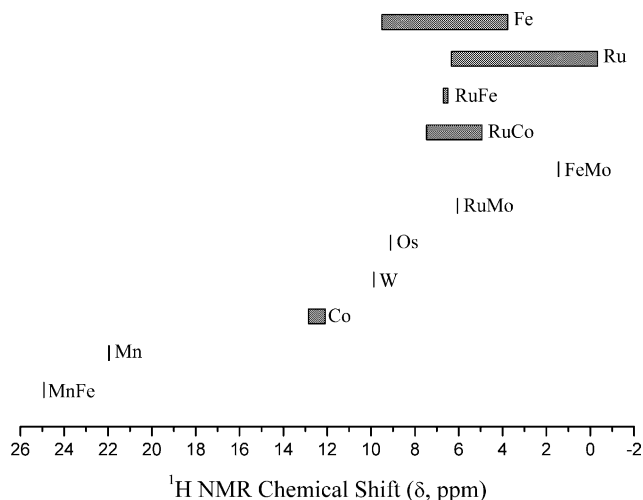


Fig. 15. Ranges of imido proton NMR signals in some transition metal clusters containing triply capping NH ligand.

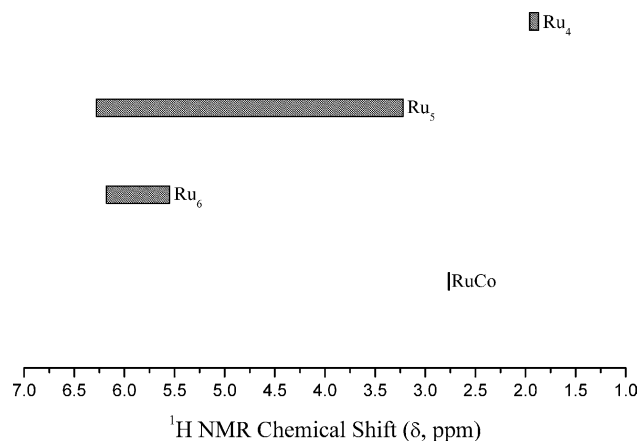


Fig. 16. Ranges of imido proton NMR signals in some transition metal clusters containing quadruply capping NH ligand.

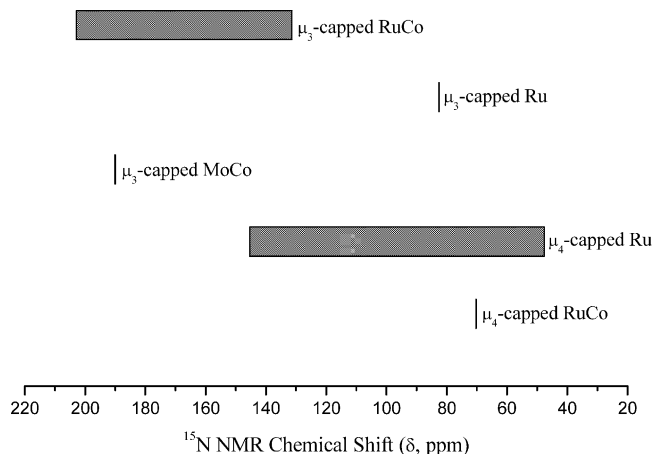


Fig. 17. Ranges of imido nitrogen ¹⁵N NMR signals in some transition metal clusters containing NH ligand.

Table 3

¹⁵N-NMR data of transition metal clusters containing μ_3 - and μ_4 -NH imido ligands

| Formula | μ_3 -NH (δ , ppm) ^a | μ_4 -NH (δ , ppm) ^a | Ref. |
|-----------------------------------------------------------------------------------------------------------------------------------------------------------|--------------------------------------------|--------------------------------------------|------|
| $\text{Ru}_3\text{Co}_2(\text{CO})_7(\mu_3\text{-CO})(\eta^5\text{-Cp}^*)_2(\mu_3\text{-NH})\{\mu_4\text{-}\eta^8\text{-C}_6\text{H}_4\text{C(H)C(Ph)}\}$ | 202.90 (76.05) | | [68] |
| $\text{Mo}_3\text{Co}_2(\eta^5\text{-Cp}^*)_3(\text{CO})_8(\mu_3\text{-NH})(\mu_4\text{-N})$ | 190.00 (76) | | [75] |
| $\text{Ru}_2\text{Co}(\text{CO})_6(\mu_3\text{-CO})(\eta^5\text{-Cp}^*)(\mu_3\text{-NH})$ | 131.40 (76.95) | | [69] |
| $\text{Ru}_3(\text{CO})_9(\mu_3\text{-CO})(\mu_3\text{-NH})$ | 82.50 (77.5) | | [77] |
| $\text{Ru}_4(\text{CO})_9(\mu\text{-CO})_2(\mu_4\text{-NH})(\mu_4\text{-}\eta^2\text{-PhC}_2\text{Ph})$ | | 47.60 (70.54) | [55] |
| $\text{Ru}_4(\text{CO})_9(\mu\text{-CO})_2(\mu_4\text{-NH})(\mu_4\text{-}\eta^2\text{-HC}_2\text{Tol})$ | | 53.13 (70.64) | [55] |
| $\text{Ru}_3\text{Co}(\text{CO})_6(\mu\text{-CO})_2(\eta^5\text{-Cp}^*)(\mu_4\text{-NH})(\mu_4\text{-}\eta^2\text{-PhC}_2\text{Ph})$ | | 70.20 (69.26) | [69] |
| $\text{Ru}_5(\mu\text{-H})(\text{CO})_9(\mu\text{-CO})_3(\eta^5\text{-Cp}^*)(\mu_4\text{-NH})$ | | 145.40 (68.26) | [69] |

^a ¹⁵NH coupling constant values in parentheses.

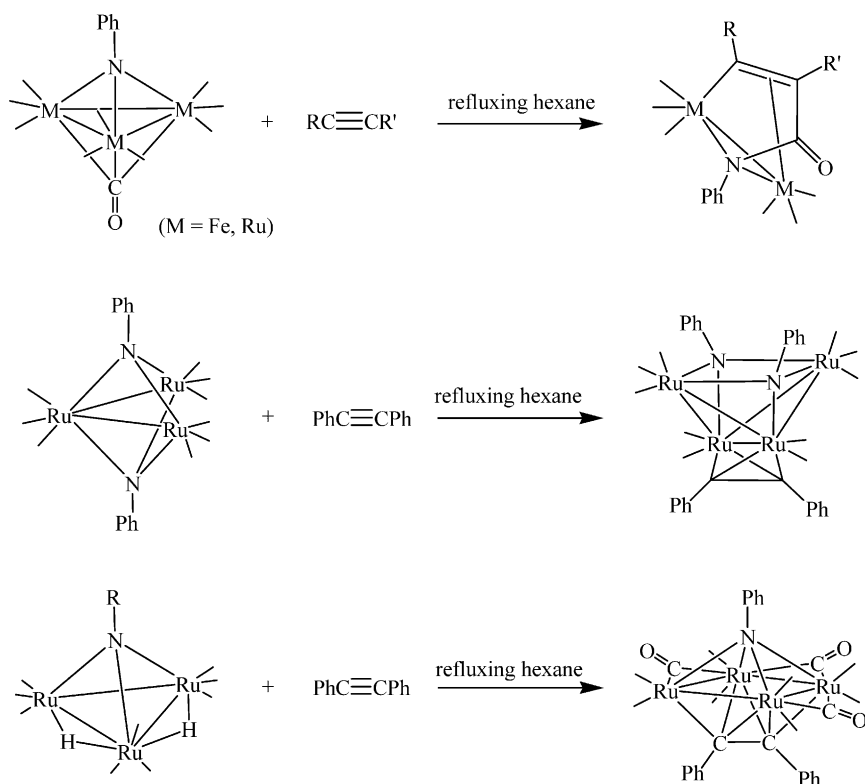
Recently, Cabeza et al. reported that the isolation of the trinuclear derivatives $[\text{Ru}_3(\mu_3\text{-NPh})(\mu_3\text{-}\eta^2\text{-PhC}\equiv\text{CC}\equiv\text{CPh})(\text{CO})_9]$ in the reaction of $[\text{Ru}_3(\mu_3\text{-NPh})(\mu_3\text{-CO})(\text{CO})_9]$ with diphenylbutadiyne. Its thermolysis leads to a mixture of binuclear metallapyrrolinone complex $[\text{Ru}_2\{\mu_2\text{-}\eta^3\text{-(PhC}_2\text{)C=CR'C(O)NPh}\}(\text{CO})_6]$ and tetranuclear complex $[\text{Ru}_4(\text{CO})_9(\mu\text{-CO})_2(\mu_4\text{-NH})(\mu_4\text{-}\eta^2\text{-(PhC}_2\text{)C}_2\text{Ph})]$ (Scheme 19). Hence, this trinuclear complex that contains coordinated alkyne is believed to be the intermediate [105].

The imido ligand is generally associated with the low valent metal clusters via a typical μ_3 -mode or a less common μ_4 -mode. However, Chi et al. discovered that

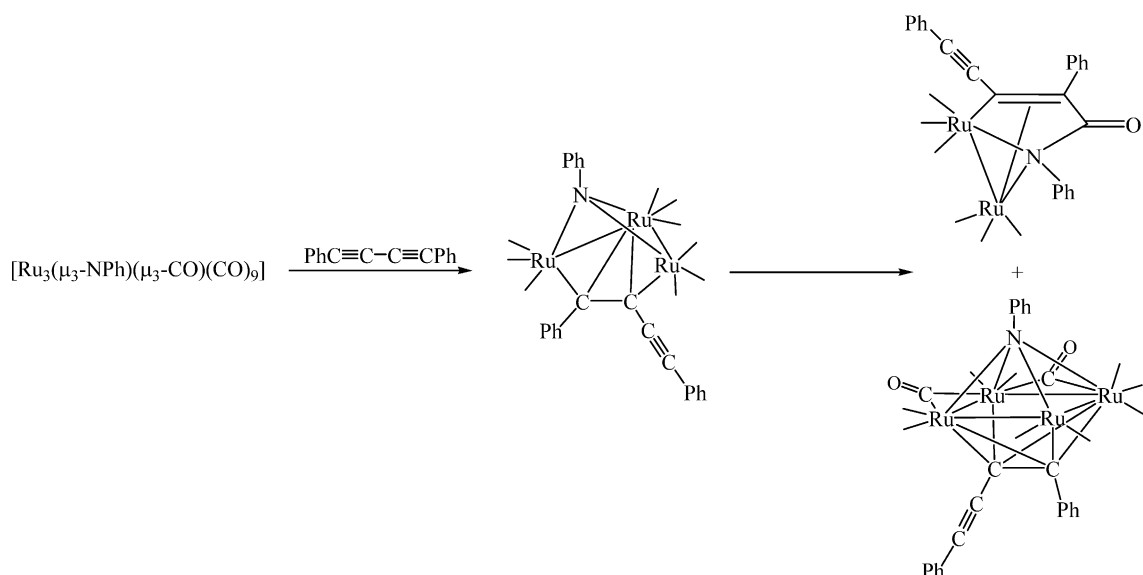
the interaction of alkynes with an imido cluster can affect the coordination mode of the imido ligand (Scheme 20) [106–108]. The first example of terminally bonded imido cluster $[\text{WRu}_2\text{Cp}^*(\text{CO})_6(\text{NPh})\{\text{C(Et)C(Et)C(CF}_3\text{)CH(CF}_3\text{)}\}]$ was isolated.

5.2. Reactions toward azo compounds

Gladfelter et al. reported that the reaction of $[\text{Ru}_3(\mu_3\text{-NAr})(\text{CO})_{10}]$ with azoarenes under CO results in the cleavage of the N–N double to produce $[\text{Ru}_3(\mu_3\text{-NAr})(\mu_3\text{-NAr}')(\text{CO})_9]$ in high yield [109,110]. In the absence of CO, the orthometallation of the azo ligand

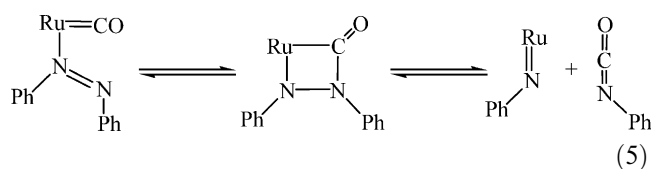


Scheme 18.



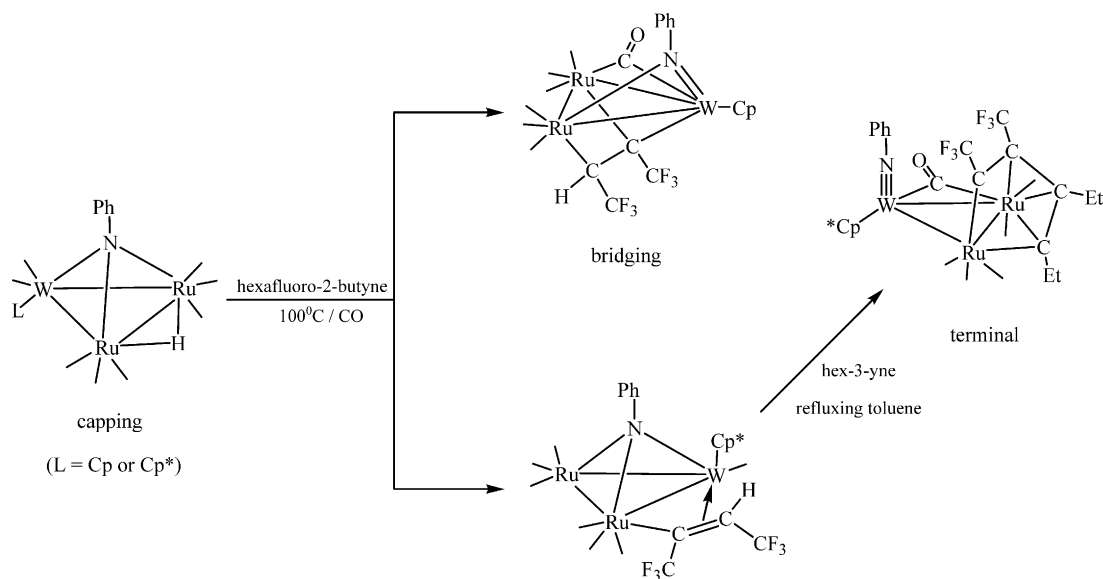
Scheme 19.

was observed (Scheme 21). The product distribution is sensitive to the *para* substituent on the azo compound, with electron-withdrawing groups favoring a N–N bond cleavage, while orthometalation is favored by electron-donating groups. The subsequent steps that lead to N=N bond cleavage are believed to involve a metathesis-like reaction of the N–N double bond with the Ru–C bond, which clearly has some π character to it (Eq. (5)). It is surprising to observe the complete selectivity in the formation of the unsymmetric bis(imido) product. None of the original imido ligand was displaced as the isocyanate. This indicates that the triply capped imido ligand is relatively inert.

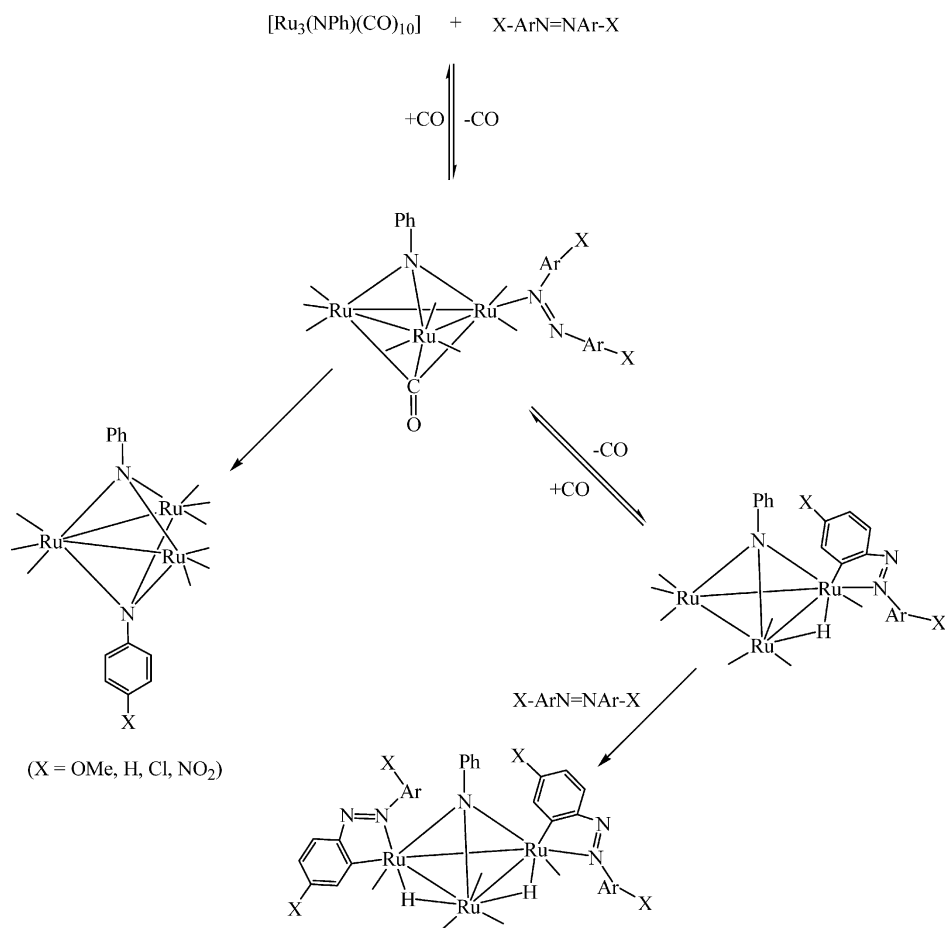


5.3. Reductive reactions

Acyl or formyl-substituted clusters $[\text{M}_3(\mu_3\text{-NPh})_x(\text{CO})_y\text{C}\{\text{O}\}\text{R}^-]$ ($\text{M} = \text{Fe}, \text{Ru}; x = 1 \text{ or } 2; y = 8 \text{ or } 9; \text{R} = \text{H}, \text{Me}, \text{OMe}, \text{Ph}$) are readily formed upon

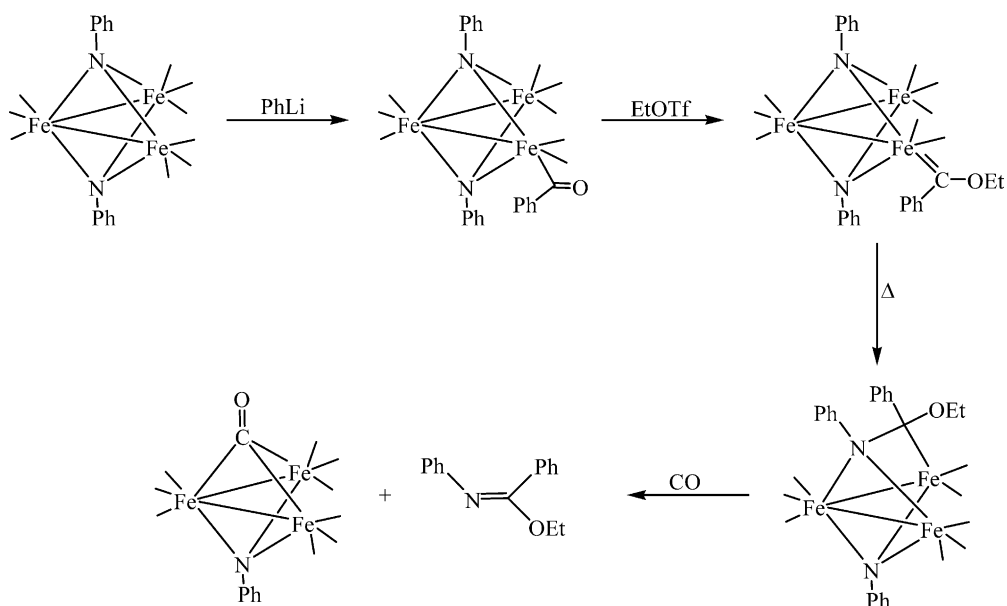


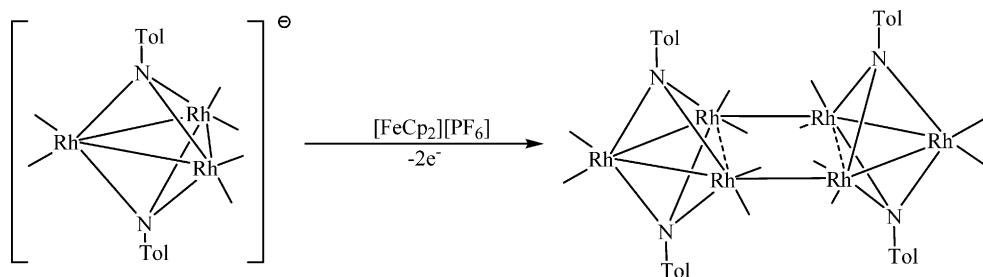
Scheme 20.



addition of the appropriate lithium reagents to the imido clusters [21,111,112]. The capping imido ligands are capable of stabilizing the trinuclear cluster frame-

work to the point of allowing the preparation of formyl, acyl, and carbene derivatives. Intramolecular imido-carbene and imido-acyl coupling reactions have been





Scheme 23.

reported whereby the acyl ligands are believed to have migrated into the imido ligands and free anilides have formed from the resultant amido clusters (Scheme 22). These reactions are believed to be closely related to the carbene-phosphinidene coupling reactions.

5.4. Other reactions

The low valent metal clusters that contain imido-capped ligands have also been found to be active in oxidation [87], substitution [113], carbonylation [89], addition [114], and photochemical reactions [81]. These reactions are relatively common and the capping imido ligands serve to retain the cluster integrity. It is noteworthy that the oxidation of $[(\text{Ph}_3\text{P})_2\text{N}][\text{Rh}_3(\mu_3\text{-NC}_6\text{H}_4\text{Me-}p)_2(\text{CO})_6]$ with $[\text{FeCp}_2][\text{PF}_6]$ gives the novel high nuclearity hexarhodium compound $[\{\text{Rh}_3(\mu_3\text{-NC}_6\text{H}_4\text{Me-}p)_2(\text{CO})_6\}_2]$ by ‘bi-edge-condensation’ (Scheme 23). This kind of cluster dimerization by oxidation is unusual.

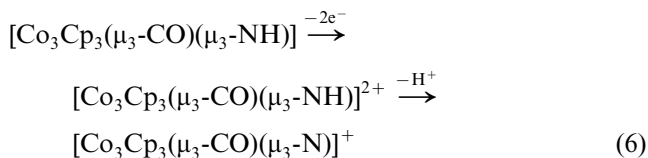
6. Electrochemical studies

A systematic electrochemical investigation was reported by Dahl et al. in the 1980s for a series of $[\text{Co}_3(\eta^5\text{-C}_5\text{H}_{5-x}\text{Me}_x)_3(\mu_3\text{-XO})(\mu_3\text{-NR})]^n$ clusters ($n = 0, +1$; $\text{X} = \text{C}, \text{N}$; $x = 0, 1, 5$; $\text{R} = \text{SiMe}_3, \text{H}, \text{CONH}_2$) that contained one π -acidic $\mu_3\text{-CO/NO}$ ligand and one π -donor $\mu_3\text{-NR}$ imido ligand [28,115,117]. The cyclic voltammetric study of clusters with mixed π -donor and π -acceptor triply capped ligands is particularly important in exploring the effects of variations in the nature of the ligands on the physicochemical properties of these clusters. Several of these mixed-ligand capped clusters exhibit rare two-electron redox processes, while others display successive one-electron oxidations and reductions. The two-electron process in the reversible interconversion of each neutral cluster to its dication or dianion is presumed to be a consequence of the cluster giving up/accepting a second electron with nearly the same or even greater facility than giving up/accepting the first electron. The addition or removal of the electrons leads to marked changes in the entire trinuclear core, which more than compensate for the

greater electrostatic repulsions that are due to the second electron. These marked changes in electrochemical response are associated with the nature of the capping ligands.

One salient feature of the redox behavior of these clusters is that the NSiMe_3 -capped cluster is both harder to oxidize and easier to reduce than a corresponding NH -capped cluster. These data are consistent with the premise that the $\mu_3\text{-NSiMe}_3$ ligand is effectively functioning as a weaker σ electron donor and stronger π -acceptor than is a $\mu_3\text{-NH}$ ligand. UV–vis spectra for clusters $[\text{Co}_3(\eta^5\text{-C}_5\text{H}_{5-x}\text{Me}_x)_3(\mu_3\text{-CO})(\mu_3\text{-NR})]$ ($\text{R} = \text{SiMe}_3, x = 0, 1, 5$; $\text{R} = \text{H}, x = 1, 5$) show that each of the NH -capped clusters exhibits a similar spectral pattern that consists of a broad band with a maximum at ca. 420 nm and a well defined shoulder between 500 and 540 nm. In contrast, the NSiR_3 -capped clusters only have one characteristic shoulder at ca. 440 nm on a sharply rising band that extends into the UV region. This spectral difference can be rationalized in terms of the π -acceptor characteristic of the Me_3SiN ligand providing greater energy stabilization of the HOMO relative to its LUMO such that the lowest energy absorption band is blue shifted to higher energy.

Electrochemical experiment also provides convincing evidence for the deprotonation of a triply bridging NH ligand to a ‘bare’ pyramidal-like nitrido-capped ligand from the electrochemically-generated dication (Eq. (6)).

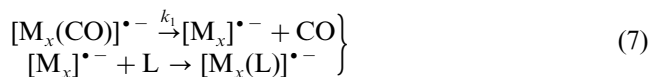


Furthermore, the isolation and structural characterization of the oxidized/reduced cluster series $[\text{Co}_3(\eta^5\text{-C}_5\text{H}_{5-x}\text{Me}_x)_3(\mu_3\text{-NO})(\mu_3\text{-NH})]^n$ ($x = 0, 1$; $n = 0, +1$) have correlated the redox-generated variations in geometry with the changes in electronic configuration [116]. This indicates that the one-electron reduction of the 48-electron monocation $[\text{Co}_3(\eta^5\text{-C}_5\text{H}_4\text{Me})_3(\mu_3\text{-NO})(\mu_3\text{-NH})]^+$ to the neutral 49-electron gives rise to a significant distortion in the distances between the cobalt atoms and a small but noticeable increase in Co-C (ring) distances for two of the three $\text{C}_5\text{H}_4\text{Me}$ ligands in

the ordered molecule. The overall distortion of the $[\text{Co}_3(\text{NO})(\text{NH})]$ core represents a clear-cut change from an idealized C_{3v-3m} geometry to an idealized C_s-m geometry. The similar changes in geometry were also observed upon the reduction of the 48-electron imido-capped $[(\text{C}_5\text{H}_4\text{Me})\text{MnFe}_2(\text{C}_5\text{H}_4\text{Me})_2(\mu_2\text{-CO})(\mu_2\text{-NO})(\mu_3\text{-NH})]^+$ monocation to its 49-electron neutral species, where an idealized C_s configuration in the 48-electron system is reduced to a pseudo- C_{3v} geometry in the 49-electron complex [76].

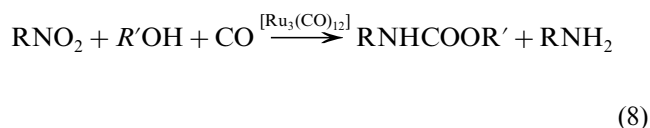
Dahl reported another bonding analysis of redox-generated changes in geometry upon formation of electron-deficient species by oxidation of triangularly bonded 48-electron metal clusters $[\text{Co}_3(\eta^5\text{-C}_5\text{Me}_5)_3-x(\eta^5\text{-C}_5\text{H}_4\text{Me})_x(\mu_3\text{-CO})(\mu_3\text{-NH})]^n$ ($x = 0, 1, 2; n = 0, +1$) [117]. The change in mean metal-metal bond distances upon the oxidation of a 48-electron cluster to the corresponding 47-electron cluster is insignificant in compare to the relevant values that have been observed in the reduction of 48-electron tricobalt clusters to their corresponding 49/50-electron clusters. This indicates that in the 48-electron tricobalt clusters mentioned above, the tricobalt antibonding character is generally much less in their HOMOs than in their LUMOs.

The triiron cluster $[\text{Fe}_3(\text{CO})_9(\mu_3\text{-NPh})_2]$ has been reported to undergo rapid and efficient electron-transfer chain (ETC) catalysis of ligand substitution [118]. Electrochemical experiments have revealed that the rate, efficiency, and selectivity of ETC catalysis are highly dependent on the nature of the capping imido ligand. Such studies demonstrate that ETC activation critically depends on the rate that anion-radical intermediate $[\text{Fe}_3(\text{CO})_9(\mu_3\text{-NPh})_2]^-$ undergoes ligand substitution in the rate-determining step (Eq. (7)). The formation of different anion radicals is correlated with differences in the electronegativity and metal-ligand bonds of nitrogen.

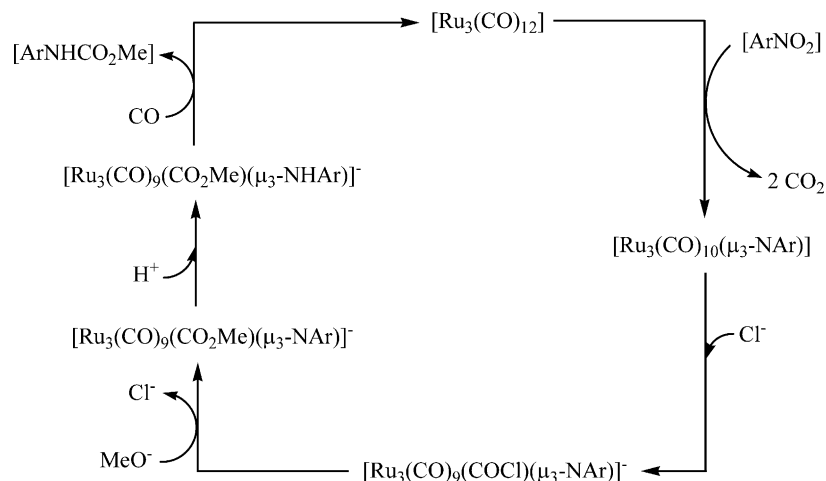


7. Catalytic properties

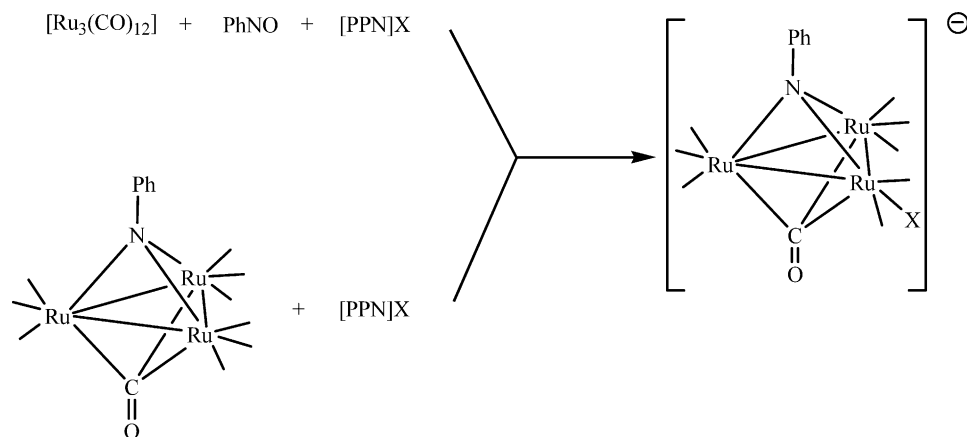
The reductive carbonylation of organic nitro-compounds is a reaction with significant synthetic and industrial interest. It avoids the use of highly toxic phosgene to prepare important industrial chemicals, such as amines, amides, oximes, urea, carbamates, isocyanates, and indoles. A number of reports have appeared on the reductive carbonylation of nitro-compounds with $[\text{Ru}_3(\text{CO})_{12}]$ as a homogeneous catalyst (Eq. (8)) [119–124].



The $\mu_3\text{-NR}$ imido-capped triruthenium metal clusters have been proposed as the intermediate of this catalytic reaction (Scheme 24), and their reactivities have been fully investigated. It has been shown that the $\mu_3\text{-NR}$ can couple with coordinated benzoyl and methoxy carbonyl groups in an intramolecular fashion to give, after oxidative degradation, benzanilide and carbamates respectively [111,112]. Furthermore, the addition of anions such as halides, hydroxides, and alkoxides has remarkable effects on the activities and selectivities of the catalytic systems [11–24]. Insights into the possible role of the halide promoters in this catalytic system has been gained by demonstrating that halides promote the formation of imido ligands on triruthenium clusters from nitroso reagents, and that they also promote the subsequent carbonylation of the imido ligands to form isocyanates. The halide substituted clusters either form



Scheme 24.



Scheme 25.

from the reaction of PhNO with $[\text{Ru}_3(\text{CO})_{12}]$ in the presence of halides or from the direct reaction of $[\text{Ru}_3(\mu_3\text{-NPh})(\text{CO})_{10}]$ with halides (Scheme 25). They have also been found to react with CO to form isocyanate under far milder conditions. The proposed sequence of events of this transformation is shown in Scheme 26. The terminal halide ligand is believed to displace one of the Ru-NPh bonds to yield an intermediate with a μ_2 -imido ligand. The nitrogen atom then adds to an adjacent carbonyl ligand to produce a coordinated isocyanate ligand, which can then be displaced by CO to yield free phenyl isocyanate and the starting cluster.

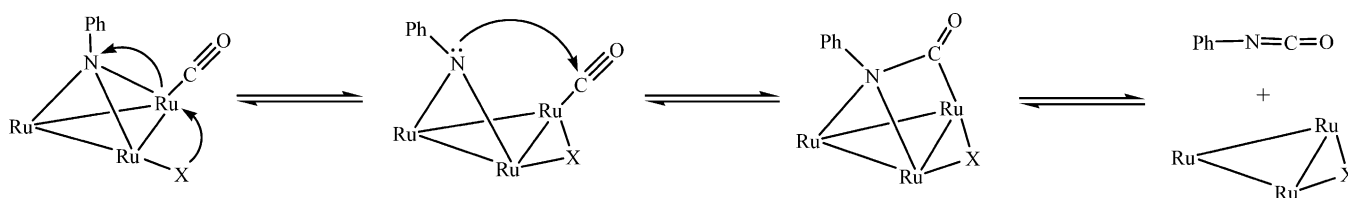
8. Concluding remarks

Low valent transition metal clusters that contain imido ligands have been known for four decades, but new synthetic routes to the imido clusters are still being developed, and an increasing number of the structures of these species are being established by X-ray analysis. Among the synthetic routes, the thermolysis and pyrolysis of nitrosyl complexes are the most efficient methods for the preparation of imido clusters (both homometallic and heterometallic). Most commonly observed is the triply capped imido cluster in which the triangular metal core is either monocapped or bicapped with imido or other electron donating ligands, such as CO , NO , or S . The quadruply capped imido

cluster is relatively unstable when compared to triply capped species, and alkynes are usually involved in the reaction as stabilizing agents. The cluster geometry is closely related to the nature of the capping ligands. In addition, the different degrees of interaction of μ_3 - and μ_4 -NH imido ligands with metals leads to a marked difference in the ^1H - and ^{15}N -NMR parameters. The ^{15}N -NMR signals of μ_4 -NH nitrogen atoms are more shielded when compared to the values that are observed in μ_3 -NH clusters. Likewise, the coupling constants for direct ^{15}N - ^1H interactions in the μ_4 -NH moieties are slightly smaller than those for the μ_3 -NH species. These characteristic values provide useful information in ascertaining whether the imido ligand is bound to three or four metal centers.

Electrochemical studies of these imido-capped clusters have revealed that the redox behavior is associated with the electron donating or accepting ability of the capping imido ligand. The cluster geometry is varied with the changes in electronic configuration, and the degrees of change depend on the antibonding characteristic of metal cluster HOMO and LUMO.

The capping imido ligands are capable of stabilizing the trinuclear cluster framework to the point of allowing the preparation of formyl, acyl, and carbene derivative through intramolecular imido-carbene and imido-acyl coupling reactions. The μ_3 -NR imido-capped triruthenium metal clusters have been proven to be the intermediates of the reductive carbonylation of nitro compounds. The halides have significant promoting



Scheme 26.

effects in the transformation of the imido ligand to isocyanate.

We believe that future research in this area will be focused on the reactivities of the imido clusters and their potential application in catalysis. The reactivity study of interactions between metal cluster bounded imido ligands and small organic molecules is especially significant, and will provide information on several important catalytic reactions that involve surface bound nitrogen atoms.

Acknowledgements

We gratefully acknowledge financial support from the Hong Kong Research Grants Council and the University of Hong Kong. Y. Li acknowledges the receipt of a postgraduate studentship (1999–2002) and a Li Po Chun Scholarship (2001–02) administered by the University of Hong Kong, and the Sir Edward Youde Memorial Fellowship (2001–02) awarded by the Sir Edward Youde Memorial Trustees.

References

- [1] J.M. Smith, R.J. Lachicotte, K.A. Pittard, T.R. Cundari, G. Lukat-Rodgers, K.R. Rodgers, P.L. Holland, *J. Am. Chem. Soc.* 123 (2001) 922.
- [2] C.G. Yiokari, G.E. Pitselis, D.G. Polydoros, A.D. Katsaounis, C.G. Vayenas, *J. Phys. Chem. A* 104 (2000) 10600.
- [3] M. Vettraino, M. Trudeau, A.Y.H. Lo, R.W. Schurko, D. Antonelli, *J. Am. Chem. Soc.* 124 (2002) 9567.
- [4] G.M. Coia, M. Devenney, P.S. White, T.J. Meyer, D.A. Wink, *Inorg. Chem.* 36 (1997) 2341.
- [5] C.-H. Kuo, F. Yuan, D.O. Hill, *Ind. Eng. Chem. Res.* 36 (1997) 4108.
- [6] Z.Y. Ding, L. Li, D. Wade, E.F. Gloyna, *Ind. Eng. Chem. Res.* 37 (1998) 1707.
- [7] W.A. Nugent, B.L. Haymore, *Coord. Chem. Rev.* 31 (1980) 123.
- [8] J.K. Brask, T. Chivers, *Angew. Chem. Int. Ed.* 40 (2001) 3960.
- [9] P.R. Sharp, *J. Chem. Soc. Dalton Trans.* (2000) 2647.
- [10] D.E. Wigley, *Prog. Inorg. Chem.* 42 (1994) 239.
- [11] L.H. Gade, P. Mountford, *Coord. Chem. Rev.* 216–217 (2001) 65.
- [12] E. Sappa, L. Milone, *J. Organomet. Chem.* 61 (1973) 383.
- [13] S. Bhaduri, K.S. Gopalkrishnan, G.M. Sheldrick, W. Clegg, D. Stalke, *J. Chem. Soc. Dalton Trans.* (1983) 2339.
- [14] A. Basu, S. Bhaduri, H. Khwaja, P.G. Jones, K. Meyer-Base, G.M. Sheldrick, *J. Chem. Soc. Dalton Trans.* (1986) 2501.
- [15] G. Gervasio, R. Rossetti, P.L. Stanghellini, *J. Chem. Soc. Chem. Commun.* (1977) 387.
- [16] W. Clegg, G.M. Sheldrick, D. Stalke, S. Bhaduri, K.S. Gopalkrishnan, *Acta Crystallogr. Sect. C* 40 (1984) 927.
- [17] R.J. Doedens, *Inorg. Chem.* 8 (1969) 570.
- [18] G. Lavigne, H.D. Kaesz, *J. Am. Chem. Soc.* 106 (1984) 4647.
- [19] G. Lavigne, N. Lugan, J.J. Bonnet, *J. Chem. Soc. Chem. Commun.* (1987) 957.
- [20] S.H. Han, G.L. Geoffroy, B.D. Dombek, A.L. Rheingold, *Inorg. Chem.* 27 (1988) 4355.
- [21] S.H. Han, J.S. Song, P.D. Macklin, S.T. Nguyen, G.L. Geoffroy, A.L. Rheingold, *Organometallics* 8 (1989) 2127.
- [22] S.H. Han, G.L. Geoffroy, A.L. Rheingold, *Inorg. Chem.* 26 (1987) 3426.
- [23] D.L. Ramage, G.L. Geoffroy, A.L. Rheingold, B.S. Haggerty, *Organometallics* 11 (1992) 1242.
- [24] F. Ragaini, J.S. Song, D.L. Ramage, G.L. Geoffroy, G.A.P. Yap, A.L. Rheingold, *Organometallics* 14 (1995) 387.
- [25] E. Koerner von Gustorf, R. Wagner, *Angew. Chem. Int. Ed. Engl.* 10 (1971) 910.
- [26] B.L. Barnett, C. Kruger, *Angew. Chem. Int. Ed. Engl.* 10 (1971) 910.
- [27] E.W. Abel, T. Blackmore, R.J. Whitley, *Inorg. Nucl. Chem. Lett.* 10 (1974) 941.
- [28] R.L. Bedard, A.D. Rae, L.F. Dahl, *J. Am. Chem. Soc.* 108 (1986) 5924.
- [29] K. Burgess, B.F.G. Johnson, J. Lewis, P.R. Raithby, *J. Chem. Soc. Dalton Trans.* (1982) 2085.
- [30] K. Burgess, B.F.G. Johnson, J. Lewis, P.R. Raithby, *J. Organomet. Chem.* 224 (1982) C40.
- [31] M.A. Andrews, H.D. Kaesz, *J. Am. Chem. Soc.* 79 (1979) 7255.
- [32] J. Banford, Z. Dawoodi, K. Henrick, M.J. Mays, *J. Chem. Soc. Chem. Commun.* (1982) 554.
- [33] Z. Dawoodi, M.J. Mays, K. Henrick, *J. Chem. Soc. Dalton Trans.* (1984) 433.
- [34] P. Michelin Lausarot, L. Operti, G.A. Vaglio, M. Valle, A. Tiripicchio, M. Tiripicchio Camellini, *Inorg. Chim. Acta* 122 (1986) 103.
- [35] E.J. Wucherer, M. Tasi, B. Hansert, A.K. Powell, M.T. Garland, J.F. Halet, J.Y. Saillard, H. Vahrenkamp, *Inorg. Chem.* 28 (1989) 3564.
- [36] M. Tasi, A.K. Powell, H. Vahrenkamp, *Chem. Ber.* 124 (1991) 1549.
- [37] B. Hansert, A.K. Powell, H. Vahrenkamp, *Chem. Ber.* 124 (1991) 2697.
- [38] H.K. Fun, O. Bin Shawkataly, R. Bin Othman, S.G. Teoh, T.S. Yeoh, *Acta Crystallogr. Sect. C* 46 (1990) 1417.
- [39] Z. Dawoodi, M.J. Mays, P.R. Raithby, *J. Chem. Soc. Chem. Commun.* (1980) 713.
- [40] S. Bhaduri, K.S. Gopalkrishnan, W. Clegg, P.G. Jones, G.M. Sheldrick, D. Stalke, *J. Chem. Soc. Dalton Trans.* (1984) 1765.
- [41] C.C. Yin, A.J. Deeming, *J. Chem. Soc. Dalton Trans.* (1974) 1013.
- [42] Y. Li, Z.Y. Lin, W.T. Wong, *Organometallics* 22 (2003) 1029.
- [43] W.Y. Yeh, C.L. Stern, D.F. Shriver, *Inorg. Chem.* 35 (1996) 7857.
- [44] W.Y. Yeh, C.L. Stern, D.F. Shriver, *Inorg. Chem.* 36 (1996) 4408.
- [45] Q.W. Liu, X. Hu, S.T. Liu, H.Q. Su, B.Y. Wang, M. Wang, *Wuji Huaxue Xuebao* 7 (1991) 202.
- [46] D.E. Fjare, W.L. Gladfelter, *Inorg. Chem.* 20 (1981) 3533.
- [47] D.E. Fjare, W.L. Gladfelter, *J. Am. Chem. Soc.* 103 (1981) 1573.
- [48] M.L. Blohm, W.L. Gladfelter, *Organometallics* 5 (1986) 1049.
- [49] P. Legzdins, C.R. Nurse, S.J. Rettig, *J. Am. Chem. Soc.* 105 (1983) 3727.
- [50] L. Scoles, B.T. Sterenberg, K.A. Udachin, A.J. Carty, *Chem. Commun.* (2002) 320.
- [51] K.K.H. Lee, W.T. Wong, *J. Organomet. Chem.* 503 (1995) C43.
- [52] K.K.H. Lee, W.T. Wong, *Inorg. Chem.* 35 (1996) 5393.
- [53] K.K.H. Lee, W.T. Wong, *J. Chem. Soc. Dalton Trans.* (1996) 1707.
- [54] E.N.M. Ho, W.T. Wong, *J. Chem. Soc. Dalton Trans.* (1998) 513.
- [55] E.N.M. Ho, W.T. Wong, *J. Chem. Soc. Dalton Trans.* (1998) 4215.
- [56] H. Schmidbaur, A. Kolb, P. Bissinger, *Inorg. Chem.* 31 (1992) 4370.

- [57] R.E. Allan, M.A. Beswick, M.A. Paver, P.R. Raithby, A. Steiner, D.S. Wright, *Angew. Chem. Int. Ed. Engl.* 35 (1996) 208.
- [58] A. Xia, A.J. James, P.R. Sharp, *Organometallics* 18 (1999) 451.
- [59] L.G. Kuzmina, J.A.K. Howard, K.I. Grandberg, G.G. Aleksandrov, V.S. Kuzmin, *Koord. Khim.* 25 (1999) 546.
- [60] A. Kolb, P. Bissinger, H. Schmidbaur, *Z. Anorg. Allg. Chem.* 619 (1993) 1580.
- [61] P. Lange, H. Beruda, W. Hiller, H. Schmidbaur, *Z. Naturforsch. Teil B* 49 (1994) 781.
- [62] S. Otsuka, A. Nakamura, T. Yoshida, *Inorg. Chem.* 7 (1968) 261.
- [63] N. Kamijyo, T. Watanabe, *Bull. Chem. Soc. Jpn.* 47 (2) (1974) 373.
- [64] H. Klein, A. Dal, S. Hartmann, U. Florke, H. Haupt, *Inorg. Chim. Acta* 287 (1999) 199.
- [65] P. Braunstein, J. Rosé, *Catalysis by Di- and Polynuclear Metal Cluster Complexes*, Wiley-VCH, New York, 1998, p. 443.
- [66] P. Braunstein, J. Rosé, *Comprehensive Organometallic Chemistry II*, vol. 10, Pergamon Press, Oxford, 1995, p. 351.
- [67] P. Braunstein, J. Rosé, *Comprehensive Organometallic Chemistry II*, vol. 10, Pergamon Press, Oxford, 1995, p. 351.
- [68] E.N.M. Ho, Z.Y. Lin, W.T. Wong, *Chem. Eur. J.* 7 (2001) 258.
- [69] E.N.M. Ho, Z.Y. Lin, W.T. Wong, *Eur. J. Inorg. Chem.* (2001) 1321.
- [70] K.K.H. Lee, W.T. Wong, *J. Organomet. Chem.* 577 (1999) 323.
- [71] E.J. Voss, M. Sabat, D.F. Shriver, *Inorg. Chem.* 30 (1991) 2705.
- [72] Y. Chi, L.K. Liu, G. Huttner, W. Imhof, *J. Organomet. Chem.* 384 (1990) 93.
- [73] V. Saboonchian, A. Gutierrez, G. Wilkinson, B. Hussain-Bates, M.B. Hursthouse, *Polyhedron* 10 (1991) 1423.
- [74] W.H. Sun, S.Y. Yan, H.Q. Wang, Y.Q. Yin, K.B. Yu, *Polyhedron* 11 (1992) 1143.
- [75] C.P. Gibson, L.F. Dahl, *Organometallics* 7 (1988) 543.
- [76] M.E. Barr, A. Bjarnason, L.F. Dahl, *Organometallics* 13 (1994) 1981.
- [77] M.L. Blohm, D.E. Fjare, W.L. Gladfelter, *J. Am. Chem. Soc.* 108 (1986) 2301.
- [78] C.W. Pin, Y. Chi, C. Chung, A.J. Carty, S.M. Peng, G.H. Lee, *Organometallics* 17 (1998) 4146.
- [79] J. Puga, R.A. Sanchez-Delgado, J. Ascanio, D. Braga, *J. Chem. Soc. Chem. Commun.* (1986) 1631.
- [80] J. Puga, A. Arce, R.A. Sanchez-Delgado, J. Ascanio, A. Andriollo, D. Braga, F. Grepioni, *J. Chem. Soc. Dalton Trans.* (1988) 913.
- [81] J.S. Song, G.L. Geoffroy, A.L. Rheingold, *Inorg. Chem.* 31 (1992) 1505.
- [82] W.Y. Yeh, C.L. Stem, D.F. Shriver, *Inorg. Chem.* 36 (1997) 4408.
- [83] P.M. Lausarot, L. Operti, G.A. Valigo, M. Valle, A. Tiripicchio, M. Tiripicchio Camellini, P. Gariboldi, *Inorg. Chim. Acta* 122 (1986) 103.
- [84] G. Gervasio, R. Rossetti, P.L. Stanghellini, *J. Chem. Res.* 334 (1979) 3943.
- [85] H. Link, D. Fenske, *Z. Anorg. Allg. Chem.* 625 (1999) 1878.
- [86] A. Decker, D. Fenske, K. Maczek, *Angew. Chem. Int. Ed. Engl.* 35 (1996) 2863.
- [87] C. Tejel, M. Bordonaba, M.A. Ciriano, F.J. Lahoz, L.A. Oro, *Chem. Commun.* (1999) 2387.
- [88] C. Tejel, Y.M. Shi, M.A. Ciriano, A.J. Edwards, F.J. Lahoz, L.A. Oro, *Angew. Chem. Int. Ed. Engl.* 35 (1996) 633.
- [89] C. Tejel, Y.M. Shi, M.A. Ciriano, A.J. Edwards, F.J. Lahoz, L.A. Oro, *Angew. Chem. Int. Ed. Engl.* 35 (1996) 1516.
- [90] C. Tejel, Y.M. Shi, M.A. Ciriano, A.J. Edwards, F.J. Lahoz, J. Modrego, L.A. Oro, *J. Am. Chem. Soc.* 119 (1997) 6678.
- [91] P. Reiss, D. Fenske, *Z. Anorg. Allg. Chem.* 626 (2000) 1317.
- [92] A.A. Danopoulos, G. Wilkinson, B. Hussain-Bates, M.B. Hursthouse, *J. Chem. Soc. Dalton Trans.* (1990) 2753.
- [93] P. Reiss, D. Fenske, *Z. Anorg. Allg. Chem.* 626 (2000) 2245.
- [94] I.L. Eremenko, A.A. Pasynskii, E.A. Vasyutinskaya, S.E. Nefedov, A.D. Shaposhnikova, O.G. Ellert, V.M. Novotortsev, A.I. Yanovsky, Yu.T. Struckov, *Metalloorg. Khim.* 1 (1988) 372.
- [95] I.L. Eremenko, A.A. Pasynskii, E.A. Vasyutinskaya, A.S. Katugin, S.E. Nefedov, O.G. Ellert, V.M. Novotortsev, A.F. Shestakov, A.I. Yanovsky, Yu.T. Struckov, *J. Organomet. Chem.* 411 (1991) 193.
- [96] S. Uriel, K. Boubekeur, P. Batail, J. Orduna, *Angew. Chem. Int. Ed. Engl.* 35 (1996) 1544.
- [97] A. Decker, F. Simon, K. Boubekeur, D. Fenske, P. Batail, *Z. Anorg. Allg. Chem.* 626 (2000) 309.
- [98] M.H. Chrisholm, D.M. Hoffman, J.C. Huffman, *Inorg. Chem.* 24 (1985) 797.
- [99] M.I. Bruce, E. Horn, P.A. Humphrey, E.R.T. Tiekink, *J. Organomet. Chem.* 518 (1996) 121.
- [100] A.J. Gordon, R.A. Ford, *The Chemist's Companion: A Handbook of Practical Data, Techniques, and References*, Wiley, New York, 1972, p. 299.
- [101] R.L. Lichter, J.D. Roberts, *J. Org. Chem.* 35 (1970) 2806.
- [102] T. Axenrod, M.J. Wieder, G. Berti, P.L. Barilli, *J. Am. Chem. Soc.* 92 (1970) 6066.
- [103] S.H. Han, G.L. Geoffroy, *Organometallics* 5 (1986) 2561.
- [104] J.S. Song, S.H. Han, S.T. Nguyen, G.L. Geoffroy, A.L. Rheingold, *Organometallics* 9 (1990) 2386.
- [105] J.A. Cabeza, I. del Rio, S. Garcia-Granda, M. Moreno, V. Riera, M.J. Rosales-Hoz, M. Suarez, *Eur. J. Inorg. Chem.* (2001) 2899.
- [106] Y. Chi, H.F. Hsu, L.K. Liu, S.M. Peng, G.H. Lee, *Organometallics* 11 (1992) 1763.
- [107] Y. Chi, D.K. Hwang, S.F. Chen, L.K. Liu, *J. Chem. Soc. Chem. Commun.* (1989) 1540.
- [108] R.C. Lin, Y. Chi, S.M. Peng, G.H. Lee, *J. Chem. Soc. Chem. Commun.* (1992) 1705.
- [109] J.A. Smieja, J.E. Gozum, W.L. Gladfelter, *Organometallics* 5 (1986) 2154.
- [110] J.A. Smieja, J.E. Gozum, W.L. Gladfelter, *Organometallics* 6 (1987) 1311.
- [111] G.D. Williams, G.L. Geoffroy, R.R. Whittle, *J. Am. Chem. Soc.* 107 (1985) 729.
- [112] G.D. Williams, R.R. Whittle, G.L. Geoffroy, A.L. Rheingold, *J. Am. Chem. Soc.* 109 (1987) 3936.
- [113] H.F. Shen, R.A. Senter, S.G. Bott, M.G. Richmond, *Inorg. Chim. Acta* 247 (1996) 161.
- [114] Z. Dawoodi, M.J. Mays, P.R. Raithby, *J. Chem. Soc. Chem. Commun.* (1981) 801.
- [115] R.L. Bedard, A.D. Rae, L.F. Dahl, *J. Am. Chem. Soc.* 108 (1986) 5933.
- [116] R.L. Bedard, A.D. Rae, L.F. Dahl, *J. Am. Chem. Soc.* 108 (1986) 5942.
- [117] M.S. Ziebarth, L.F. Dahl, *J. Am. Chem. Soc.* 112 (1990) 2411.
- [118] T.M. Bockman, J.K. Kochi, *J. Am. Chem. Soc.* 109 (1987) 7725.
- [119] F. Ragaini, A. Ghitti, S. Cenini, *Organometallics* 18 (1999) 4925.
- [120] D.K. Mukherjee, B.K. Palit, C.R. Saha, *J. Mol. Catal.* 91 (1994) 19.
- [121] J.D. Gargulak, A.J. Berry, M.D. Noirot, W.L. Gladfelter, *J. Am. Soc.* 114 (1992) 8933.
- [122] S. Cenini, M. Pizzotti, C. Crotti, F. Ragaini, F. Porta, *J. Mol. Catal.* 49 (1988) 59.
- [123] S. Cenini, C. Crotti, F. Ragaini, F. Porta, *J. Org. Chem.* 53 (1988) 1243.
- [124] S. Cenini, F. Ragaini, *Catalytic Reductive Carbonylation of Organic Nitro Compounds*, Kluwer Academic Publishers, The Netherlands, 1997.